ABSTRACT

SOME MECHANICAL PROPERTIES
OF CHERRY BARK AND WOOD

by Robert G. Diener

This study was initiated to study the mechanical behavior of fruit tree bark to applied stresses. Since the green wood is closely associated with the bark in the tree limb green wood was also included. Also since, during mechanical harvesting different frequencies of vibration are used, the frequency of the applied stress was also considered. Tests were limited to a single variety and species: Montmorency Cherry, Prunus Crasus.

All tests were conducted under controlled temperature and humidity conditions in a testing chamber. Maximum strength of bark specimens was determined from tensile loading in a pneumatic testing machine. Elastic and viscous properties of bark and green wood specimens were measured using elastic and viscoelastic flexure theory. Three loading techniques were used for the flexure tests. These tests were (1) loading at a slow constant strain rate using a simple beam arrangement (2) free vibration as a cantilever beam and (3) forced vibration as a simple beam. As a check on the theory and experimental technique

several specimens of aluminum, Plexiglas, and white pine wood were included in these tests.

Approximate and exact equations for determining the viscoelastic modulus from dynamic flexure were derived. The accuracy of these equations was described graphically in terms of measured variables. From this it was possible to use the approximate equations with a negligible amount of error.

From a transverse microscopic section of bark the tissue appeared to be arranged in four major radial layers. These layers consisted of a non functioning phloem, a functioning phloem, and two periderms which made up about 10, 65, 12, and 12 per cent of the total thickness respectively.

The strength of bark was very dependent on the direction of the applied force. Maximum longitudinal and tangential strengths for the three inner bark tissues were about 640 and 70 pounds per square inch respectively. The outer periderm strengths were about 980 and 3250 pounds per square inch in these respective directions. Longitudinal cambium shear strength was about 30 pounds per square inch.

The storage modulus of bark was very sensitive to frequency of the applied stress and varied from about 10,000 to 40,000 pounds per square inch over a frequency range of

about 10^{-3} to 10^{-2} cycles per second. The storage modulus of green wood varied a lesser amount from about 500,000 to 700,000 pounds per square inch over a slightly larger frequency range. The loss tangents of bark and wood were about .15 and .04 respectively.

Approved F H Buelow
Major Professor

Approved Carl W. Hall
Department Chairman

SOME MECHANICAL PROPERTIES OF CHERRY BARK AND WOOD

By

Robert G. Diener

A THESIS

Submitted to
Michigan State University
in partial fulfillment of the requirements
for the degree of

DOCTOR OF PHILOSOPHY

Department of Agricultural Engineering

1965

ACKNOWLEDGMENTS

The author sincerely appreciates the assistance of all who have aided in this study. He is especially appreciative, however, for the counsel and guidance provided by his major professor, Dr. F. H. Buelow (Agricultural Engineering), during this graduate program.

To the other members of the guidance committee, Dr. B. A. Stout (Agricultural Engineering), Dr. G. E. Mase (Metallurgy, Mechanics and Materials Science), Dr. S. K. Ries (Horticulture) and Dr. E. A. Nordhaus (Mathematics), the author expresses his deepest gratitude for their time, professional interest, and constructive suggestions.

Dr. L. E. Malvern (Metallurgy, Mechanics, and Materials) and Dr. L. W. Mericle (Botany and Plant Pathology) made helpful comments during various stages of this study. Mr. James Cawood and his staff in the Agricultural Engineering Research Laboratory assisted in the development of the experimental apparatus.

TABLE OF CONTENTS

LIST OF TABLES

LIST OF FIGURES

LIST OF APPENDIX TABLES

INTRODUCTION

Mechanization of harvest operations in recent years has been a practical solution to the problem of the high cost of hand labor facing the American fruit grower. In many cases the cost of harvesting has amounted to as much as half the total cost of production. Also, hand labor is not always available when needed, and managing and housing laborers requires additional time and expense.

Several techniques have been introduced to enable the grower to mechanize harvest operations such as use of mobile platforms, picking tubes, picking spindles and tree vibration. However, the first three methods require selectivity in their use and do not cover a large area of the tree in a single application. Among the various means and principles which have been tried for detaching the fruit, vibration appears to be the simplest and most practical method.

Although vibratory mechanical harvesting is less expensive than hand harvesting, some resultant damage to the fruit and tree must be tolerated. Fruit damage occurs in the detachment and collection phases when the fruit come

into contact with each other or collide with limbs during the fall through the tree. Halderson (1963) categorized the resultant tree damage into three parts; those produced on the limb, trunk, and root systems. However by the use of an accelerometer attached to the tree during shaking, he found all motion to cease a few inches below ground level and concluded that root damage was negligible.

Injury to the limb occurs by the breaking of fruit bearing spurs, fracture of small limbs from whipping action during shaking, and rupture of the bark tissue in the shaker clamp area. Adrian and Fridley described bark injury as occurring while locating the clamp on the limb, clamping with excessive radial pressures, and improper alignment of the shaker boom with the limb causing excessive longitudinal stresses in the bark. Additional stresses in the tangential direction may also be produced if the shaking machine moves while vibrating the limb or if the limb tries to assume a path of oscillation which is not parallel with the applied shaking force. However, as reported by Adrian and Fridley, what bark damage occurred could be tolerated in view of the savings resulting from mechanical harvesting. Then it was discovered that a Ceratocystis Canker was entering the bruised bark tissue. Devey, et al. (1962), described this canker as a fungus disease which originates in bruised bark tissues and rapidly spreads to healthy tissues. In a relatively short

time the fungus would kill the diseased limb and in many cases cause the death of the entire tree. Chaney (1964) reported that orchards so infected may be expected to die out completely within ten years. As a result of loss in production caused by this infection cooperative studies were initiated by the United States Department of Agriculture and the University of California Department of Agricultural Engineering to determine allowable shaker clamp stress that could be applied without injuring the bark tissue. From these studies an upper limit of safe radial stress was found as well as general indications of the relative magnitudes of maximum longitudinal and tangential bark strengths.

Since mechanical properties of a material such as strength and also elastic modulus and internal damping determine the behavior to applied stresses, it was felt that the study reported in this thesis should cover these additional properties. Also, since a wide range of frequencies is used in mechanical harvesting, it was considered advisable that behavior be studied on the basis of the frequency of the applied stress. Furthermore, since the bark and green wood are closely associated in the tree, it was felt that the study should be extended to cover green wood as well.

Objective

The objective of this study was to investigate physical properties and mechanical response to applied stresses in bark and green wood tissues. Specific objectives of this study were:

1. Develop or adapt from existing equations the necessary mathematical formulas for description of mechanical behavior of bark and green wood under applied stresses.

2. Develop the necessary experimental procedures and equipment to measure and record the physical properties and mechanical properties such as strength, elasticity, and damping of the materials under study.

3. Develop a testing chamber having controlled temperature and humidity conditions in which to have the testing facilities and to conduct the experiments.

RELATED LITERATURE

Structural and Mechanical Properties of Plant Tissue

The smallest structural unit of plant tissue is the cell. The cell is composed of a non-protoplasmic rigid wall and an inner cytoplasmic fluid. Roelofsen (1959) described cell walls as having largely supportive and protective functions and thus the walls determine the shape of the cell and the texture. Two types of wall structures are present in living plants, a primary wall and a secondary wall. Usually living cells which carry out life processes have only a primary wall whereas non-living cells, whose function is primarily supportive, have an additional secondary wall. Primary walls are composed of a fine mesh network of cellulose fibrils which is filled with pectic and hydrophilic compounds; in woody tissues they are filled with lignin and in cutinized walls with waxes and cutin. The pectic compounds constitute the major portion of the middle lamella between adjacent walls of the cells. In secondary walls most of the cellulose present is crystalline cellulose. In the heavier secondary wall, the cellulose fibrils are grouped into coarser

branching strands which are encrusted with pectins, hemicelluloses and lignins. In walls that are pure cellulose, such as the secondary wall of cotton fibers, the spaces are filled with water. Lignin is one of the most important wall substances in woody tissues. This polymer encrusts the wall providing a stiffening and protective function.

Mechanical Properties of Plant Cells.--Plant cells are classed as parenchyma, collenchyma or sclerenchyma cells depending on their wall structure and function. Parenchyma cells are living cells. They are soft, elastic and are capable of large plastic deformations at certain periods during growth (Heyn, 1940). Collenchyma cells are similar to parenchyma with the exception of some thickening at the wall edges which contribute some strength to the tissue. In sclerenchyma cells a large secondary wall is present inside the primary wall. This secondary wall may become so thick that the central cavity almost disappears. Both primary and secondary walls in cells exhibit elastic behavior, but primary walls are much more flexible. Meyer et al. (1963) described the tensile strength of secondary walls as comparable to that of spring steel. Frey-Wyssling (1952) reported that primary walls were capable of up to 50 per cent extension as compared to only about two per cent for the secondary walls in fiber cells. Meyer (1950) thought the differences in behavior between primary and secondary walls was due to

the large amounts of amorphous cellulose and pectic compounds in primary walls as contrasted to the crystalline cellulose and lignins in secondary walls. He also stated that the presence of lignin does not affect the tensile strength, but increases the compression strength by preventing the cellulose strands in the walls from buckling under compressive loadings. However, Frey-Wyssling (1952) suggested that the encrusting substances in and between the cells and the arrangement of the fibrils accounted for the amount of elasticity and strength and not the crystalline and amorphous regions in the fibrils themselves. He also stated that the pectins, hemicelluloses and amorphous cellulose are very sensible to swelling with water and that as a result elasticity and plasticity in the fibers depend markedly on moisture content. Frey-Wyssling (1952) found that ultimate stress in cotton hairs could be related to the spiral angle of the fibrils in the cells. He found that the ultimate strength increased as the fibrils became orientated more in the direction of pull. Under high stresses cellulose fibers and other cells often show slip planes. Meyer (1950) explains failure under these conditions as a slipping or fracture of the molecular chains. In native fibers where the chains are long, failure occurs by rupture of the chain. In artificial fibers where the chains are shorter he suggests that failure occurs by slipping between chains and hence these fibers are subject to humidity content giving them a low "wet strength."

For the purposes of comparison of some of the mechanical properties of plant fiber cells and other materials Table 1 is presented below from data presented by Meyer (1950), Frey-Wyssling (1952), and Esau (1965).

TABLE 1.--Mechanical properties of plant fibers and some other materials.

Material	Average property in psi x 10^{-3} and strain in in/in.			
	Tensile strength	Compression strength	Elastic modulus	Ultimate strain
Collenchyma (fiber)	14.0			.02
Sclerenchyma (fiber)	28.4			.01
Cotton (fiber)	60	7	1,100	
Wool (fiber)	25	-	280	
Nylon (fiber)	110	17	1,000	
Concrete	190	-	2,800	
Wood	14	12	1,750	
Aluminum	35	38	9,800	
Steel	140	<140	28,000	

In woody tissues having thickened secondary walls, Frey-Wyssling (1952) thought that the instability of the cell shape determined the mechanical response of the cell to applied stresses. He also thought this to be the reason for anisotropy in wood. Wood also has definite isotropic directions with respect to the principal fiber orientations. For example, the average ratio of elastic moduli magnitudes

in wood in the tangential, radial and longitudinal directions is about 1:2:20 respectively, (U.S.D.A. Wood Handbook, 1955). Frey-Wyssling (1952) summarized and reported on studies made by other investigators of the anisotropy in Douglas fir and spruce. They found that the elastic modulus measured between the principal orientations of the fibers varies in a complicated pattern with changes in angular location. They also found that under compressive loading, the large trachied cells failed by collapsing or structural instability. The walls of the cells deformed in an "S" shape and the edges of the walls remained at right angles to each other.

Moisture content in wood is defined as the ratio of water to dry matter (U.S.D.A. Wood Handbook, 1955). The moisture present in wood is divided into two parts: (1) free water in cell cavities and in intercellular spaces and (2) absorbed water in the capillaries of the walls. The fiber saturation point is reached when all the free water is absent at about 30 per cent moisture content. Mechanical properties in wood are affected by moisture content. Wood increases in strength as it drys. Longitudinal compressive strengths for 12 and five per cent wood, for example, are about two and three times the strength of green wood respectively. The strength of green wood does not begin to increase with drying, however, until the fiber saturation point is reached. The change in strength has

been associated with moisture content in the following relation (U.S.D.A. Wood Handbook, 1955) as $\log S_3 = \log S_1 + (M_1-M_3/M_1-M_2) \log S_2/S_1$ where S_1,S_2 and S_3 are the strengths at moisture contents M_1,M_2 and M_3. Changes in temperature have a slight effect on wood. Generally wood strength increases with decreasing temperature. The opposite is also true. It is estimated this strength variation is about one-half per cent per degree F. from a base temperature of 77 degrees F. When wood is exposed to temperatures above 150 degrees F. it is permanently weakened.

Structural and Rheological Properties of Fruit Tree Bark

The non-technical term "bark" refers to the tissues in the stem outside the vascular cambium. The bark is composed of the phloem, an inner food conducting tissue, and the periderm, an outer protective tissue.

Arrangement of Bark Tissues.--The periderm consists of three tissue layers. The outer cork layer, a middle single cell layer of cork cambium cells and an inner layer of loosely packed parenchyma cells, which sometimes is not present.

The phloem is generated from the vascular cambium in an outward radial direction. The vascular cambium also produces xylem or wood cells to the interior. Generally, less phloem cells are produced than xylem and

the crushing of the phloem annually by new growth makes it much thinner than the woody part of the stem. Phloem is composed of several specialized cells such as sieve cells, fibers, and parenchyma. The sieve cells are long, tubular cells which form the food conducting tissues of the phloem. Parenchyma cells are found both at random in phloem tissue and in radial rays as ray parenchyma. Only a few layers of phloem cells next to the vascular cambium actually function in a given season. The rest are termed non-functioning phloem (Esau, 1965).

Schneider (1945) studied the seasonal changes of peach and cherry phloem. He found sweet cherry produced a new band of phloem each spring to function for the summer. In the fall the new sieve tubes became plugged and the tissue became non-functioning. During each growing season fibers matured in the phloem of the previous year, and fissures occurred along the rays. He also found that less crushing of the old cherry phloem occurred than in some other species with the result that cherry bark was much thicker than peach bark, for example, where the old phloem is completely crushed.

Mechanical Properties of Bark.--Adrian and Fridley (1963) studied bark injury in prune trees as related to shaker clamp design. They reported that bark on the tree could safely withstand a radial pressure of 250 pounds.

per square inch without rupture of inner phloem cells. Rupture was indicated by a hairline crack in the functioning phloem thought to be caused by air oxidizing the tissues in the injured cells. They found the tangential shear strength of these barks to be about 100 pounds per square inch. Longitudinal strength of bark was found to be about four times the tangential strength.

Brown (1965) conducted tests on almond and olive trees to find the effect of moisture content and normal (radial) pressure on the shear strength of bark at the cambium layer. He found that in general bark with high moisture content had low shear strength and bark with low moisture contents had high shear strengths. Shear strength was also found to be affected by the normal pressure depending on the moisture condition of the bark and variety. At moisture contents less than about 130 per cent an increase in normal pressure caused an increase in the cambium shear strength. These shear strengths were in the order of 140 to 200 pounds per square inch for normal pressures of 60 to 300 pounds per square inch. At moisture contents above 160 per cent, increase in normal pressure did not produce a corresponding increase in the shear strength of the bark, and for some varieties shear strength decreased. He suggested that to reduce injury during shaking, it would be advisable to harvest when the moisture content of the bark is at a lower level.

Concepts in Viscoelasticity and Materials

Owing to the tremendous importance of the mechanical properties of synthetic high polymers, the science of viscoelasticity has been developed largely in the last 25 years. These materials have remarkable properties which permit them to be used as rubbers, plastics, and fibers to replace materials of plant and animal origin and for new uses which were impossible before. These organic compounds are formed from hydrocarbons and their derivatives with almost infinite variations in molecular structure and resulting mechanical properties. Unsaturated hydrocarbons undergo polymerization reactions in which molecules couple together to form extended chains. The term high polymer (Sienko and Plane, 1961) is any of these large molecules containing recognizable repeatable units which form extended chains.

Polymers are formed in leaf tissue of plants where carbon dioxide and water are combined to form the sugar, and glucose. Thousands of glucose molecules unite to form large molecules of cellulose and starch. The cellulose constitutes the framework of the plant while starch serves as a food material.

Viscoelastic Behavior of Materials.--The theory of viscoelasticity, developed to explain the behavior of high polymers, allows mathematical representation of such

phenomena as stress relaxation during loading, retarded elasticity, creep and non-recoverable deformation. Even metals and glass fibers show a slight degree of viscous behavior under creep, relaxation, and sinusoidal testing. While these materials are primarily elastic these tests yield valuable information about the structure and behavior of the material. Polymers, however, exhibit a high degree of viscoelastic behavior in tests of the material. In crystalline high polymers, the crystals are rigid for all practical purposes while the amorphous regions are only rigid and brittle at temperatures below the amorphous "brittle point" (Alfrey, 1948). At higher temperatures these amorphous regions have a viscous and rubbery behavior.

Frey-Wyssling (1952) summarized and reported on studies done by other investigators on the mechanical behavior of cellulose fibers. These investigators found the tensile strength and modulus of elasticity of native cellulose fibers to be as high as the finest steels. Their highest experimental values approached the theoretical strength of a stretched rope of primary valence chains. High values were found to occur with low moisture content, low temperatures, and good orientation of the fiber. They found the large plastic deformation to occur only through consolidation and orientation of the amorphous regions. When extensions reached this point of consolidation, the fiber was rather completely crystallized, and failure occurred.

Techniques in Viscoelasticity.--It is common to represent a viscoelastic material with a mechanical model of springs, dashpots, and frictional elements in order to write a mathematical description of the behavior. These models are useful in one-dimensional studies of strain rate, creep, and stress relaxation. The one-dimensional model may be extended by use of the Correspondence Principle into a three dimensional stress-strain tensor (Bland, 1960). However, this leads to very complicated expressions for higher parameter models having three or more elements, and is useful only for homogeneous materials having simple shapes.

The behavior of viscoelastic materials may also be studied by applying a sinusoidal stress to the material and observing the resultant strain. The behavior of a specific viscoelastic model may also be studied in this way by replacing the stress and strain components in the constitutive equation with the corresponding sinusoidally varying components of stress and strain. The resulting equation may then be solved directly for the elastic modulus by obtaining the stress-strain ratio. The elastic modulus obtained in this way is called the complex modulus of elasticity. The complex modulus is usually arranged in its real and imaginary parts of vectors which represent the elastic and viscous elements respectively.

Viscoelastic Studies in Agricultural Products.--
Viscoelastic theory has more recently been applied to agricultural products in an attempt to describe their behavior. Mohsenin (1962) et al. studied creep in apple fruit using a Kelvin and a Maxwell model in series. They also recognized the importance of strain rate. Zoerb and Hall (1960), and Finney and Hall (1964) used Maxwell models in parallel arrangements to represent stress relaxation in agricultural products. Zoerb used a two element model to represent pea beans and Finney used a four element model for potatoes. Both studied the effect of strain rate on the rate of stress relaxation after loading ceased. They observed that at slower loading rates less stress relaxation resulted in a given time than that for higher rates. It is obvious here that the material is relaxing in the loading phase. At high loading rates, the material cannot relax as much in the loading phase; therefore, this occurs in the relaxation phase. As a further step, Zoerb and Finney might have plotted the relaxation time constants against loading rate to determine what relations existed. Interestingly, Zoerb found no relation between moisture content of pea beans and relaxation time. However, he noted an increase in loading force with an increase in moisture content which demonstrated a viscous effect.

Finney (1963) presented a comprehensive introduction to use of models to represent viscoelastic behavior in his Doctoral Thesis.

Testing of Hard Viscoelastic Materials

Relatively stiff materials such as wood fibers approach the rigidity of the testing apparatus and as such are not suitable for testing in sandwich or block geometry for measurement of pure shear. Rather, these materials are more suitably tested as long, thin strips in tension, thin rods in torsion or as beams in flexure.

Tension and torsion testing are sometimes not practical because of difficulties in gripping the specimen, due to low strengths of the material in the radial direction as compared to the longitudinal direction. Also it is often difficult to measure the relatively small displacements resulting from the applied stresses by direct methods such as the use of strain gages. Indirect methods must then be used by measuring the displacement of an element strained in series with the specimen being tested.

Flexure testing is frequently more desirable since this method permits large displacements without rupturing the material. In addition this method permits moving of the supports to adjust the amount of force applied to the specimen for a given displacement.

Dynamic testing techniques should be very helpful in testing semi-rigid materials. These tests are usually

fast, non-destructive, and give good results. By using rapid loading rates these tests can provide information about the material behavior for higher frequencies of applied stresses. In addition, cyclic testing in flexure, for example, bends the specimen in both forward and reverse directions, thus averaging the properties across the section. This often leads to more consistent results.

Theory of Flexure Testing for Rigid Viscoelastic Materials

Static Testing. For a simply supported beam with a center load P, the elementary elastic equation for average bending stress σ is

$$\sigma = \frac{3PL}{4bh^2} \tag{1}$$

and for Young's modulus of elasticity, E, is

$$E = \frac{PL^3}{4Ybh^3} \tag{2}$$

where E and σ are in units of pounds per square inch, P is the applied force in pounds, L is the distance between the supports in inches, Y is the displacement at the center of the beam in inches and b and h are the width and depth of the beam respectively, in inches.

However if the material under test is viscoelastic in behavior, then time must also be considered and the resulting stress and modulus become $\sigma(t)$ and $E(t)$

respectively. A generalized stress equation of this type has been proposed by Ferry (1961) for a Maxwellian material under a constant loading rate R as

$$\sigma(\varepsilon,t) = R\int \tau H[1-\exp(-t/\tau)]\, d\tau \qquad (3)$$

This equation represents a spectrum of Maxwell models each contributing a stress E and a relaxation time between τ and $d\tau$. τ is defined as the ratio of the dashpot constant η to the spring constant E. The term $H(\tau)$ is a function of the relaxation time τ and is generally called the spectrum of relaxation time. This term replaces the E's of the individual models. The variables H and τ are determined experimentally by loading the material at different strain rates and long term relaxations. However, of more importance, the time derivative of the ratio of the stress to the loading rate R in equation (3) is equal to the relaxation modulus E(t). The relaxation modulus is defined as the ratio of the relaxation stress to the strain at which relaxation is carried out (Alfrey, 1948). However, Chang (1964) has shown that the relaxation modulus can also be measured by taking the tangent modulus of the loading curve at time t. This is a useful relation since E(t) has already been related to the storage modulus, $E'(\omega)$, by Ferry (1961), in the relation

$$E'(\omega) \approx E'(1/t) \qquad (4)$$

This relation is possible for low frequencies or short relaxation times since the relaxation and storage moduli curves are mirror images of each other in the time and frequency axes respectively. Since both $E(t)$ and $E'(\omega)$ are measures of stored elastic energy, a dynamic measurement at frequency ω is equivalent to a transient one at $t = 1/\omega$.

Nonresonant Dynamic Testing.--The storage modulus $E'(\omega)$ and the loss modulus $E''(\omega)$ components of the viscoelastic modulus E^* are most simply written

$$E'(\omega) = E^* \cos\delta \tag{5}$$

$$E''(\omega) = E^* \sin\delta \tag{6}$$

where δ is the phase angle between the applied stress and the resulting strain. A convenient way to measure these moduli would be to apply a sinusoidally varying force to the material and observe the modulus E^* and the phase angle δ. If the material is purely viscous the displacement will lag the applied stress by a phase angle of 90 degrees. For pure elastic response the phase angle is zero. Viscoelastic materials fall somewhere between these two extremes. However, considerable difficulty is usually encountered in measuring the phase angle, δ, accurately.

Koppelmann (1858) tested Plexiglas in this way using cantilever beam geometry. In this case the modulus, E^*, was replaced by $|f|/h'|x|$, where f and x were the peak

values of applied force and resulting displacement at the end of the beam respectively and h' was a form factor depending on the geometry of the beam. In the case of a cantilever beam

$$h' = bh^3/4L^3 \qquad (7)$$

where b, h, and L were the width, depth, and free length of the beam respectively. The beam was driven by a rocker arm. One end of the rocker arm was attached to the beam by a wire and the other end of the arm was driven by a sinusoidally varying force. By the use of two small mirrors, one at the rocker arm pivot and one attached to the sinusoidal driver, Koppelmann was able to determine the phase angle from the images traced on a high speed, light sensitive film strip.

Resonance Testing.--Resonance testing techniques use the frequency and relative amplitudes of the resonance condition and as such are capable of measuring response at much higher frequencies than either static or dynamic techniques. The use of resonance techniques in measuring the behavior of materials at high frequencies are usually referred to as sonic testing. Sonic testing techniques are very suitable for testing beams in flexure. This method requires very small deflections and as such there is no danger of exceeding the limits of linear behavior in

the material or the assumptions made in the derivation of the flexure equations.

The basic relation for flexural vibrations in beams is given by Timoshenko (1921) in the equation

$$EI \frac{\partial^4 y}{\partial x^4} + \frac{\gamma A}{g} \frac{\partial^2 y}{\partial t^2} = 0 \qquad (8)$$

where E is the elastic modulus, I is the inertia of the cross seetion, γ is the density of the material, g is acceleration due to gravity and y and x are distances measured in the depth and length directions of the beam respectively. By assuming a solution of the form

$$y = D (A' \sin \omega t + B' \cos \omega t)$$

the well known expression for the natural frequency, f_n, for flexural vibrations in beams is expressed as

$$f_n^2 = \frac{1}{K} E \qquad (9)$$

where E is the modulus of elasticity in pounds per square inch, K is a beam constant and f_n is the observed natural frequency in cycles per second. The beam constant, K, is given by the relation

$$K = (2\pi)^2 A\gamma L^4 / k_m^4 \, Ig \qquad (10)$$

where L is the length of the beam and k_m is a modal constant based on the beam geometry and the particular mode of vibration. Modal constants listed by Timoshenko (1955)

for the first three modes of vibration are: for a cantilever beam, 1.875, 4.694 and 7.855 respectively and for a free beam simply supported at its nodal points, 4.730, 7.835 and 10.996 respectively. The nodal points are locations along the length of the beam which are stationary during flexural vibration of the beam at a particular mode.

Church (1964) has given the nodal locations as a non-dimensional ratio of the distance of the node from the end of the beam to the total length of the beam. For beams having different boundary conditions at the ends of the beam, such as the cantilever, the particular end of the beam from which measurement is to be made must be specified. For a cantilever beam the nodal positions as measured from the free end are: first mode, 1.0, second mode 0.226, third mode, 0.499 and 0.132. For a free beam which is simply supported, the nodal locations are symmetrical and may be measured from either end of the beam. The nodal positions are: for the first mode, 0.224 and 0.776, for the second mode, 0.132, 0.500 and 0.868, for the third mode, 0.094, 0.356, 0.644, and 0.906.

Timoshenko (1921, 1922) first recognized the effect of forces present in beams due to shear and rotation inertia and developed a new flexure equation to include these terms. Goens (1931) used the Timoshenko equation to develop an approximate correction expression for shear and rotation inertia. The Goens correction factor, T, was

used to calculate a corrected resonance frequency f_c from the observed resonance frequency f_n by the relation

$$f_c = f_n \cdot \sqrt{T} \tag{11}$$

However, in practice, the Goens equation was not easy to calculate, since the solution for T involved an iterative solution and a prior knowledge of the elastic modulus, E. Picket (1945) developed a more usable equation for the Goens correction factor T for flexural vibration of beams and cylinders. This relation is

$$T_n = 1 + \left[C_{1n} (r/\ell)^2 \quad \frac{-C_{2n} (r/\ell)^4}{1 + C_{3n}(r/\ell)^2} \right] \tag{12}$$

where the subscript, n, refers to the particular mode; C_1, C_2, and C_3 are constants, r is the radius of gyration and ℓ is the length of the beam. In a rectangular beam the ratio r/ℓ is equal to the ratio of the depth squared to twelve times the length and for a cylinder the ratio is equal to the ratio of the diameter to four times the length. The constants calculated by Picket, C_{1n}, C_{2n}, and C_{3n}, for the first three modes are: for n = 1, 88.12, 1572, and 92.61 respectively; n = 2, 229.81, 9984, and 223.6 respectively; and n = 3, 446, 38,372, and 438.3 respectively. It can be seen from equation (10) that the value of T is always slightly larger than 1.00 and becomes larger when the frequency is increased, but remains approximately equal to one for values of r/ℓ less than 0.005.

In recent years investigators have used various forms of equations (10), (11) and (12) to measure the modulus of elasticity, E, in materials using resonant flexure testing. Hearmon (1958), for example, measured Young's modulus in wooden beams, 18 to 20 inches long with nearly square cross section, using forced resonant vibration. In these tests Hearmon supported the free beams at the nodal points by two threads. Hearmon used a coil, driven by a signal generator, to drive the beam through the use of a small steel shim attached to the end of the beam. He used a shim and coil at the other end of the beam to measure the resulting amplitude which was displayed on an oscilloscope screen. The resonant frequency was determined as that frequency which resulted in the maximum amplitude of the driven beam. Hearmon found very good agreement for calculated values of E from different modes in his tests. At higher modes the value of T became significantly large. For example, in a typical sample, with a first mode resonance at 85 cycles per second the value of T was only 1.007, however, at the 16th mode, at 5365 cycles per second, the value of T increased to 1.682. Hearmon also corrected for moisture content variations in his specimens by using the relation

$$f_a = f_b(1-0.004\Delta M) \qquad (13)$$

where f_b and f_a were the resonant frequencies in cycles per

second before and after a change in moisture content, ΔM, in per cent.

Bair (1964) used free vibration of hardboard using cantilever beam geometry in an attempt to measure the effect of moisture content on Young's modulus of elasticity, E, and the logarithmic decrement, Δ. Vibrations were caused by lightly tapping the beam. The resulting motion was displayed on an oscilloscope screen using a method similar to that used by (Hearmon, 1958). From the frequency and the rate of decay of the wave form, Bair was able to calculate Young's modulus and the logarithmic decrement respectively. The logarithmic decrement, Δ, was calculated using the relation

$$\Delta = \frac{1}{n} \ln x_o/x_n \qquad (14)$$

where the ratio x_o/x_n was the initial amplitude to the amplitude n cycles later. Bair found that a linear relation existed between both E and the logarithmic decrement with respect to the moisture contents from zero up to 20 per cent. For spruce and oak, Kollmann (1960) found that the logarithmic decrement generally increased with an increase in moisture content, but not in a linear relation, up to moisture contents of 40 per cent. He noted a large drop in the logarithmic decrement at moisture contents from about 6 to 10 per cent. In addition, the logarithmic decrement did not increase for increases in moisture content above 40 per cent.

In a study of rubber-like materials Nolle (1948) extended the flexure solution for the elastic modulus equation (9), to the viscoelastic case. In his solution, Nolle assumed the material could be represented by a spring and viscous element in parallel. By use of solution for a similar a.c. resonant circuit and assuming small values of damping, he developed the two approximate equations for the storage modulus, $E'(\omega)$ and the loss modulus, $E''(\omega)$.

These relations were

$$E'(\omega) = K(V_o^2 + (\Delta V)^2/2) \tag{15}$$

$$E''(\omega) = KV_o\Delta V \tag{16}$$

where K was a constant involving the mass and dimensions of the beam as well as other constants in equation (9), V_o was the observed natural frequency, and ΔV was the observed resonance frequency band-width at .707 of the resonance frequency amplitude.

Horio and Onogi (1951) developed a solution similar to that by Nolle by adding a damping term, $\eta I \frac{\partial^5 y}{\partial x^4 \partial t}$ to the original flexure equation given by Timoshenko, equation (8). They also assumed only small values of damping in deriving the approximate solutions. These solutions were identical with those by Nolle except that the constant, 1/2, in the equation for the storage modulus was replaced by a smaller value, 1/8. This change is insignificant for low values of damping.

Bland and Lee (1955) developed an exact solution using a completely general viscoelastic law rather than the specific model used by Nolle for the determination of the viscoelastic modulus. Their solution used the amplitude and the stress-strain phase difference of the beam at resonance. A specific case of the general solution was developed to cover the case of small damping and which required only the measurement of the beam resonances for several different lengths of the beam. Another modification of the original solution allowed for solution with an end load on the beam. As a result of laboratory tests they concluded that reasonable accuracy could be obtained with Nolle's equations for small damping.

THEORETICAL ANALYSIS

Development of the Complex Modulus of Elasticity Equations

Before using the equations for forced beam vibration developed by Nolle (1948), it was decided to (a) develop these equations using theory of elementary vibrations and beam mechanics for a two parameter viscoelastic model and extend this solution to cover the case of free beam vibrations; (b) develop a second formulation of the same equations without making the usual assumptions for small damping; and (c) derive error terms for the above two sets of expressions for the storage and loss moduli in terms of the measured quantities; the frequency bandwidth ratio $\Delta\omega/\omega_{nd}$ and the logarithmic decrement Δ. These error terms would be of benefit since the investigator can immediately determine his error for higher damping when using the approximate equations without actually calculating values of the complex modulus.

Viscoelastic moduli for small damping.--For this derivation the two parameter model shown in Figure 1 is proposed to represent the material.

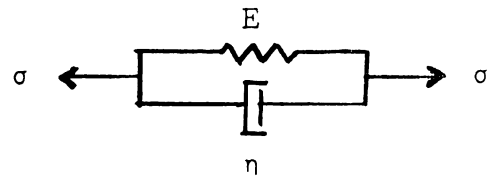

Figure 1. A two parameter Kelvin viscoelastic model containing elastic and viscous elements.

Under an applied tensile stress, σ, a material represented by this model would yield a constitutive equation of the form

$$\sigma = E\,\varepsilon + \eta\,\frac{d\varepsilon}{dt} \tag{17}$$

where E is the elastic modulus of the material in psi., η is the damping constant in units of pound seconds per square inch, and ε is the resultant strain in units of inches per inch. If we assume the material to be excited by a sinusoidal stress the resultant stress σ and strain ε may be represented by

$$\sigma = \sigma_o e^{i\omega t} \quad \text{and} \quad \varepsilon = \varepsilon_o e^{i(\omega t-\delta)}$$

where ω is the frequency in radians per second, t is the elapsed time in a cycle and δ is the phase angle between the stress σ and the strain ε. If this stress is now applied to a Kelvin material the resultant stress-strain ratio may be shown to be

$$\sigma/\varepsilon = \frac{\sigma_o e^{i\delta}}{\varepsilon_o} = E - i\eta\omega \tag{18}$$

From the above expression the real and imaginary parts of the elastic modulus may be written as the storage modulus

$E'(\omega)$ and the loss modulus $E''(\omega)$ where

$$E'(\omega) = E \quad \text{and} \quad E''(\omega) = \eta\omega \tag{19}$$

In the solution obtained by Nolle (1948) it was assumed that

$$E'(\omega) = E + \eta\omega \text{ and } E''(\omega) = \eta\omega \tag{20}$$

so that

$$E'(\omega) = E + E''(\omega)$$

By using a different formulation of the complex modulus as presented in equation 19, together with the theory of vibrations and beam mechanics, one can derive a similar set of expressions similar to equations 15 and 16 developed by Nolle (1948). In using an electrical analogy Nolle (1948) replaced mass with inductance, damping force with resistance and the spring force with the reciprocal of the capacitance.

The behavior of a spring mass system having a small amount of damping which is driven by a sinusoidal force has been studied in detail and is presented in numberous vibration texts. This system as shown in Figure 2.

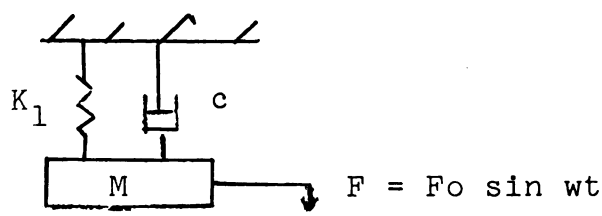

Figure 2.--Forced vibration of a damped spring-mass system.

It is represented by the equation

$$\frac{d^2(\varepsilon)}{dt^2} + \frac{c}{M}\frac{d\varepsilon}{dt} + \frac{K_1\varepsilon}{M} = \frac{F_o \mathrm{Sin}\omega t}{M} \qquad (21)$$

where ε is the displacement of the mass center at any time, t, c is the damping constant in pound seconds per inch, K_1 is the spring constant in pounds per inch, M is the mass in pound (seconds)^2 per inch and ω is the radian frequency. It has also been shown that for small amounts of damping and using the maximum displacement as a criteria of resonance the two following relations will be true:

$$\omega_{nd}^2 = \omega_n^2 (1-2\eta'^2) \qquad (22)$$

$$\Delta\omega/\omega \approx 2\eta' \qquad (23)$$

where $\Delta\omega$ is the frequency bandwidth at 0.707 of the maximum amplitude, ω_{nd} is the damped natural frequency, ω_n is the undamped natural frequency and η' is a dimensionless term known as the damping ratio.

Equation 22 may now be easily rewritten in the form of a series equation as

$$\omega_n^2 = \omega_{nd}^2(1 + 2\eta'^2 + 4\eta'^4 + 8\eta'^8 -- + -- n\eta'^n) \qquad (24)$$

If the usual assumptions for small damping are made, terms of η' higher than the second power are ignored and equations 23 and 24 are combined, the relation that results is

$$\omega_n^2 \approx (1 + \frac{\Delta\omega^2}{2\omega_{nd}^2})\ \omega_{nd}^2 \qquad (25)$$

For this system ω_n may also be expressed by the ratio K_1/M. A similar relation also exists resulting from

beam theory as discussed by Timoshenko (1921, 1922, 1961), where the natural frequency of a vibrating beam, ω_n, in radians per second, may be represented by the relation $\omega_n^2 = E/H$ where E is the Young's modulus of the beam in flexure and H is the beam constant which is given by the relation

$$H = KT_n \tag{26}$$

where the values of K and T_n are given by equations 10 and 12, respectively.

Thus the constants for a spring-mass system and a beam undergoing flexural vibration at the same frequency may be related by the equation

$$\omega_n^2 = \frac{K_1}{M} = \frac{E}{H} \tag{27}$$

Therefore from equation 25, the storage modulus $E'(\omega)$ may be represented by

$$E'(\omega) = H\omega_{nd}\left(1 + \frac{\Delta\omega^2}{2\omega_{nd}^2}\right) \tag{28}$$

This is the same as equation 15 found by Nolle (1948). By an argument similar to that used for equation 27, a relation may be written for the damping constant c in the form

$$\frac{c}{M} = \frac{\eta}{H} \tag{29}$$

where η is also a damping constant, but in units of pound seconds per square inch.

From equations 19 and 29 the expression for the loss modulus, $E''(\omega)$, becomes

$$E''(\omega) = c\omega_{nd}$$

By use of the relations $c/c_c = \eta'$, given by Thompson (1964), where c_c is the critical damping constant in units of pound seconds per square inch, and the relations $c_c = 2M\omega_n$ and $M = H$,

$$E''(\omega) = 2H\omega_n\omega_{nd}\eta' \tag{30}$$

If η' is small, equations 23 and 30 may be combined to give the relation

$$E''(\omega) = H\ \omega_{nd}^2\left(\frac{\Delta\omega}{\omega_{nd}}\right) \tag{31}$$

Equations 28 and 31 developed in this manner are identical to equations 15 and 16 developed by Nolle (1948).

For the case of free damped vibrations of a spring-mass system the following two equations have been presented by Thompson (1964), which are analogous to equations 21 and 23. The free vibration relationships are

$$\omega_{nd}^2 = \omega_n^2(1-2\eta'^2) \tag{32}$$

and $$\Delta = 2\pi\eta'/\sqrt{1-\eta'^2} \tag{33}$$

where Δ is the logarithmic decrement.

By a completely analogous method to that used in the case for forced vibrations similar solutions for storage and loss modulus may be derived for the case of free vibrations to give the following equations:

$$E'(\omega) = H\ \omega_{nd}^2\ (1 + \frac{\Delta^2}{2\pi^2}) \tag{34}$$

$$E'(\omega) = H\ \omega_{nd}^2\ (\frac{\Delta}{\pi}) \tag{35}$$

Viscoelastic moduli for large damping.--Equations will now be derived for the determination of the viscoelastic moduli in beams subjected to forced and free vibration without the assumption that $\eta' >> 1$. However, owing to the nature of equation 22 the restriction is imposed that $\eta' \leq 0.700$.

Therefore, a new equation is now derived for the case for high damping in a manner similar to that used by Thompson (1964) for equation 23 where

$$\frac{\Delta\omega}{\omega n} = 2\eta' \sqrt{1 + \eta'^2} \tag{36}$$

and by letting $\lambda = \Delta\omega/\omega_n$ equation 36 can easily be arranged into the form

$$\eta' = (\sqrt{1 + \lambda^2} - 1)/2 \tag{37}$$

If the expression for η' is then substituted in equation 22, ω_n becomes

$$\omega_n = \frac{\omega_{nd}}{\sqrt{2 - \sqrt{1 - \lambda^2}}} \tag{38}$$

This equation cannot be solved directly for ω_n since λ is also a function of ω_n. However, since this equation is already in the form $x = f(x)$, it can be easily solved for ω_n by using iteration procedures to a specified interval

of convergence such as 10^{-6}, so that for all practical purposes this becomes an exact solution.

Thus the storage modulus becomes

$$E'(\omega) = H\omega_n^2 \tag{38}$$

where the value of ω_n is given by equation 38. The storage modulus $E''(\omega)$ may now be represented by use of equations 30 and 37 as

$$E''(\omega) = H\ \omega_n\ \omega_{nd}\left(\sqrt{1-\lambda^2}-1\right) \tag{39}$$

where values of ω_n and λ are known from equation 38 and the value of $\Delta\omega$.

For the case of free vibrations, equation 33 may be rewritten in the form

$$\eta' = \frac{1}{\sqrt{4\pi^2\ \Delta^2 + 1}} \tag{40}$$

From equation 32, ω_n can be written

$$\omega_n = \frac{\omega_{nd}}{\sqrt{1-2/(4\pi^2/\Delta^2 + 1)}} \tag{41}$$

The storage modulus may now be written for free vibration as

$$E'(\omega) = \frac{H\omega_{nd}^2}{(1 - 2/(4\pi^2/\Delta^2 + 1)} \tag{42}$$

and the loss modulus becomes

$$E'(\omega) = \frac{2H\omega_n\omega_{nd}}{\sqrt{4\pi^2/\Delta^2 + 1}} \tag{43}$$

Error terms for the approximate solutions. The error resulting from using the approximate solutions may be

calculated directly from the equations presented in the preceding two sections. However, it was felt that a graphical presentation of the measured variables Δ and $\Delta\omega/\omega_{nd}$ versus per cent error would be of decided advantage over this procedure. In order to keep the same basis of comparison between the forced and free vibration solutions, values of Δ and $\Delta\omega/\omega_{nd}$ were generated from the same value of η'. Values of η' were varied from zero to 0.700 in increments of .01. Values of Δ were calculated from equation 33 and values of $\Delta\omega/\omega_{nd}$ were calculated from the relation

$$\Delta\omega/\omega_{nd} = \frac{2\eta\sqrt{1+\eta^2}}{\sqrt{1-2\eta^2}}$$

The previous solutions for the elastic moduli were redefined in terms of the measured variables Δ and $\Delta\omega/\omega_{nd}$ and the damping ratio η'. The results of these calculations are presented graphically in Figures 3 and 4.

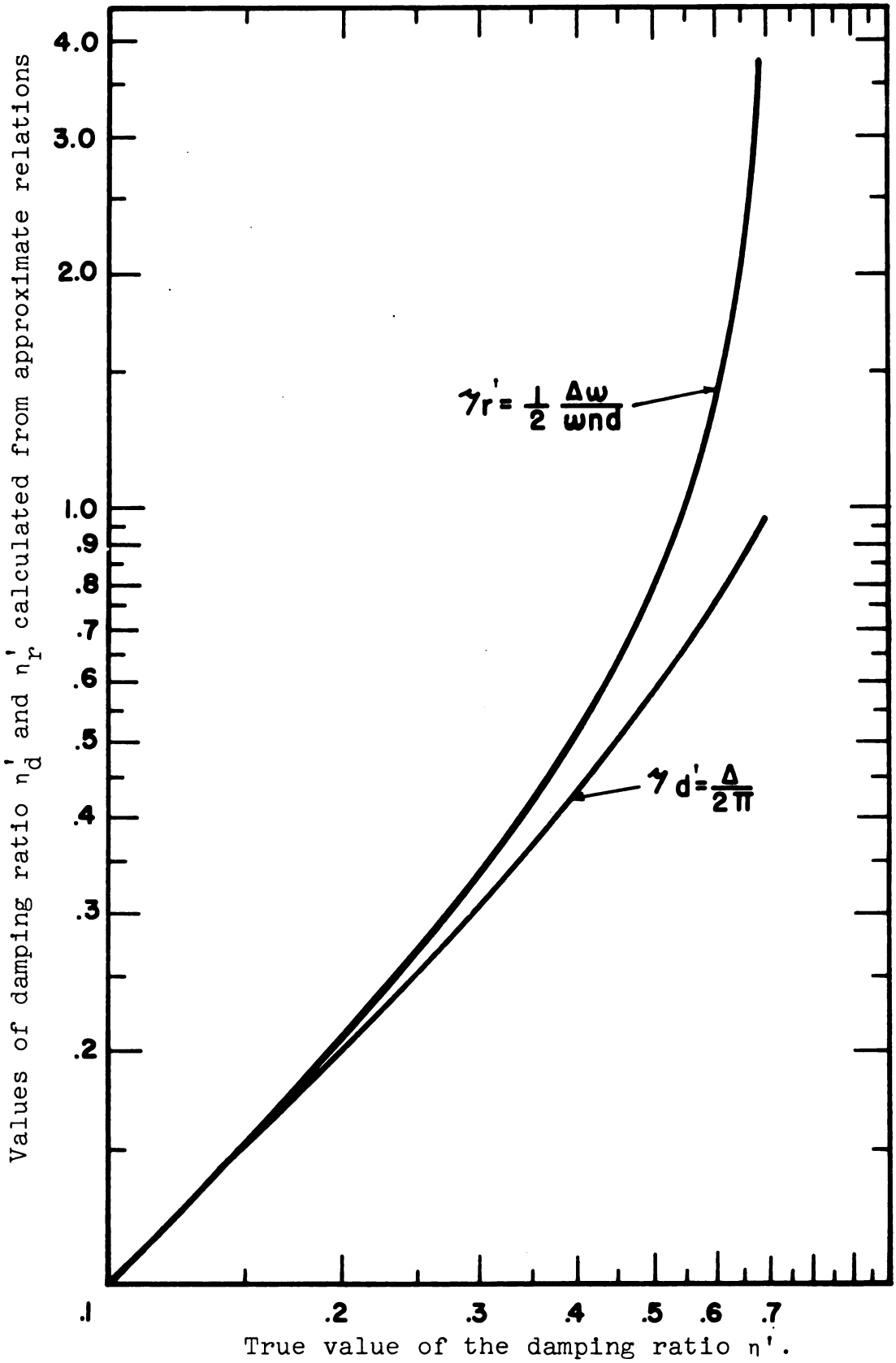

Figure 3.--Variation between true values of the damping ratio and the values calculated using the approximate equations.

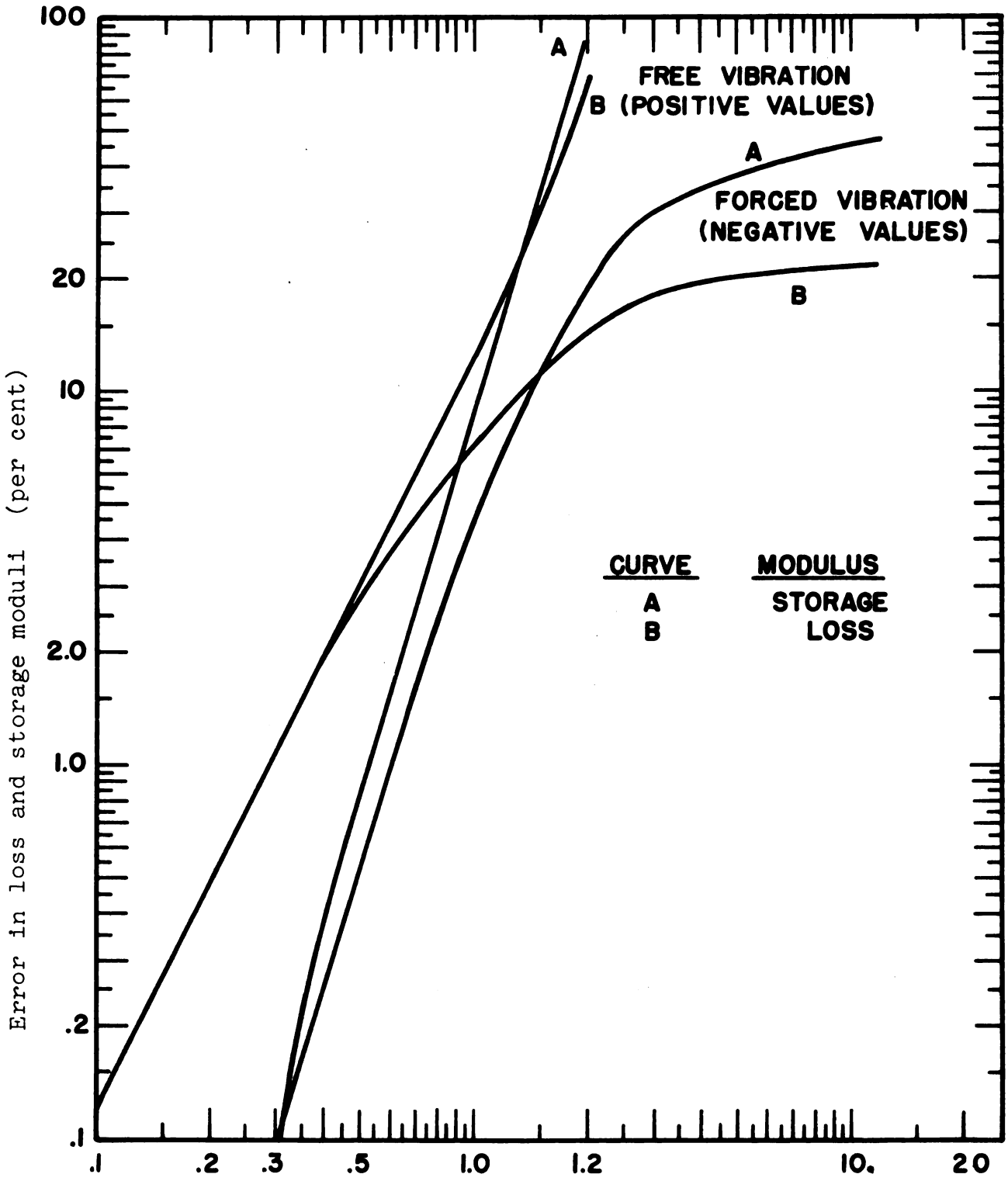

Figure 4.--Error resulting from using the approximate equations to calculate the loss and storage moduli.

LABORATORY STUDIES

To initiate a study of the physical and rheological properties of fresh bark and wood tissue, it was first necessary to assemble suitable testing facilities to measure these properties. Also it was recognized from preliminary tests that these tissues were viscoelastic in behavior and as such would be considerably influenced by temperature and humidity conditions. In an effort to reduce the effects of these variables a testing chamber was constructed to provide environmental control and house the instrumentation.

Testing Chamber

After preliminary calculations it was decided that a chamber six feet wide, eight feet long and seven feet high would be large enough to conduct the tests in and yet would not be too difficult in which to maintain controlled conditions with the equipment available. The frame of the chamber was constructed of two by two inch studding covered on both sides with one-eighth inch plywood. Fiberglas was used as insulation in the walls, ceiling, and floor of the chamber.

An air conditioner located in the lower front corner of the chamber was used to control the temperature. A deflection duct was fitted to the air conditioner to direct the cool air toward the top of the chamber to minimize temperature gradients and to reduce air movement in the area where the samples were to be tested. Moisture was introduced by releasing low pressure steam through a horizontal 20 inch length of one-half inch pipe. The pipe had small holes drilled at one inch spacings along the top. A small piece of copper tubing was connected on the low pressure end of the manifold to drain away the water condensate. The manifold was located near the floor at the rear of the chamber to allow the steam to rise and diffuse through the air before entering the air conditioner. The controls for the temperature and humidity systems were located at the testing area in the chamber. Thus when the specified conditions were set on the thermostat and the humidistat it was assured that these conditions would be met in the immediate area where the sample was to be tested. A humidistat operated solenoid in the steam line controlled the amount of steam entering the chamber.

During operation the temperature was maintained at 72 ±3 degrees F. and the humidity was held at about 75 per cent.

Maximum Strength Tests

As a preliminary part of the study of the mechanical properties of bark and green wood, bark specimens were subjected to a series of strength tests. In these studies the maximum tensile strength of bark in the longitudinal and tangential directions and the maximum longitudinal shear strength of the cambium layer were measured. Because of its higher tensile strength, the rupture strength of green wood was not measured in this study since the forces required were beyond the capacity of the testing machine. Maximum strength of wood is more easily determined by obtaining the so called rupture modulus from a bending test.

Measurement of the Maximum Tensile Strength.--For these tests bark specimens, one inch wide and ten inches long, were cut from the tree using a rectangular steel cutting frame. Then the samples were cut into necked specimens, four inches long, using a specially prepared cutter. The specimens were loaded in tension using the Bellows Valvair pneumatic testing machine shown in Figure 5. This machine is capable of producing forces in tension and compression of about 300 pounds at constant strain rates which may be varied from near zero to about 100 inches per minute. Specimens tested using this machine were held by two specially designed vices shown

Figure 5.--General view of testing apparatus.

in Figure 6. Each vice had about one square inch of clamping surface. The jaws were designed with horizontal serrated surfaces to reduce slipping. Specimens were loaded at a constant strain rate of about 1.5 inches per minute and the resulting force was measured by a Baldwin-Lima-Hamilton U-1B 50 pound capacity load cell and recorded by a Mosley 135 X-Y recorder. Displacement was measured using a dial gage indicator as shown in Figure 6. An event marker on the X-Y recorder was used to record the observed displacement intervals.

Measurement of the Longitudinal Cambium Shear Strength.--In this study the apparatus described in the preceding section was also used to measure the cambium shear strength. Specimens of bark and green wood tissue, with the cambium intact, were cut from whole limb sections which had been removed from the tree. The test specimens were about one-half inch thick, one inch wide and 5 inches long. The thickness of the woody part of the specimen was cut so as to be about equal to the thickness of the bark. This was done to prevent a moment from developing in the shear plane when a tensile force was applied. A sample prepared for testing is shown in Figure 7.

Measurement of Elasticity and Damping

In the measurement of elastic and damping properties of bark and green wood, freshly collected sections were

Figure 6.--Necked bark specimen loaded in tension using the pnuematic testing machine.

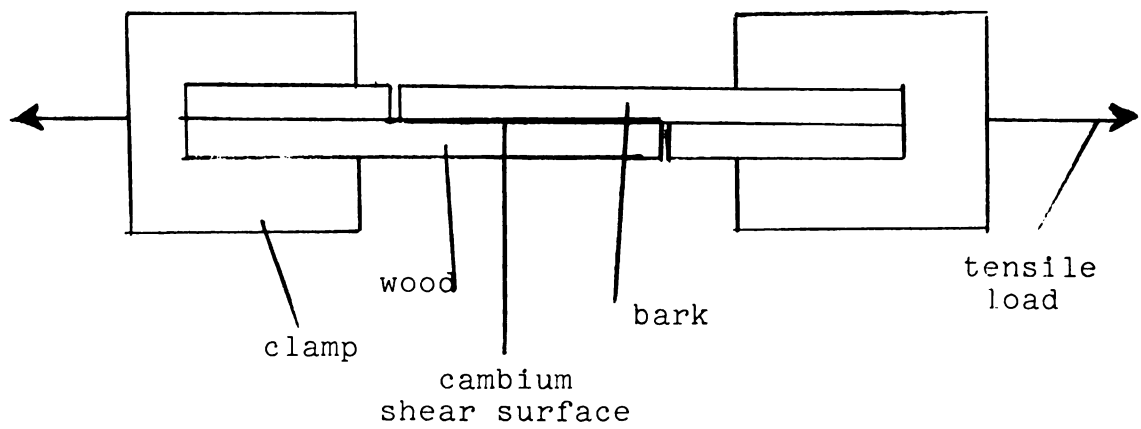

Figure 7.--Sketch of the bark and wood specimen used to determine maximum longitudinal cambium shear strength.

tested as beams using elastic and viscoelastic flexure theory. These sections were about 0.2 inch deep, one inch wide and ten inches long. The thickness of the bark sections varied slightly depending on the age.

To measure the effect of frequency of the applied stress, three separate testing techniques were used: static loading, free vibrations, and forced vibrations. However, before testing any bark or green wood specimens, several check specimens of aluminum, Plexiglas, and white pine wood were tested to check the accuracy of the experimental apparatus and to gain experience in testing techniques. These check specimens were about the same size as the bark and green wood beams, but were machined to very uniform dimensions.

Static Tests.--Static tests were conducted by loading the specimen as a simply supported beam as shown in Figure 8. The force was applied at a constant loading rate of 0.05

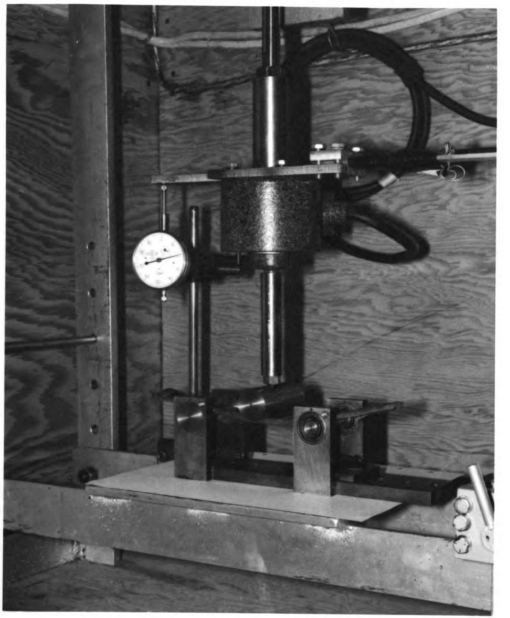

Figure 8.--Bark specimen supported as a simple beam subjected to bending stresses.

inches per minute. Owing to the low forces resulting from this type of loading, additional amplification of the load cell output was provided by using a Brush strain gage bridge amplifier. The beam support frame as shown in Figure 8 was constructed with one movable support for force-displacement ratio. The beam rested on two steel shafts which were force fitted through the supports. In addition, the shaft of the movable support was held in a ball bearing mount to prevent horizontal constraints from occurring during bending of the beams.

Tests were conducted in two parts: (1) a constant strain rate loading, and (2) followed by a stress relaxation test while the specimen was held at constant deformation. The time base of the recorder was used for both deformation and relaxation measurements. During the loading phase displacements were measured using a dial gage at the load cell. The observed displacements were recorded using an event marker on the X-Y recorder.

Free Vibration Tests.--In the free vibration tests the specimen was clamped at one end while the other end was free to vibrate as shown in Figure 9. Free vibrations were initiated by lightly tapping the beam. The resulting vibrations were detected by positioning a magnetic coil under a small steel shim which was fastened to the bottom of the beam. The resulting voltage from the coil was

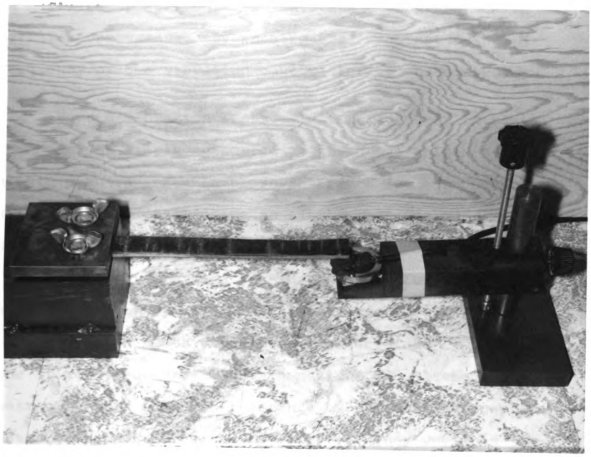

Figure 9.--Bark specimen rigidly fixed as a cantilever beam for free vibration tests.

amplified using a Tektronix preamplifier shown in a rack mounting in Figure 5. The resulting wave was displayed on an oscilloscope screen. The wave was photographed with an oscilloscope camera. By knowing the sweep speed the frequency of the vibration could later be calculated.

Forced Vibration Tests.--In forced vibration tests the beam was simply supported at the nodal points by two aluminum knife edges as shown in Figure 10. The beam was excited by positioning an electromagnetic driver coil under a small metal shim fastened on one end of the beam. The resulting vibrations were detected at the opposite end of the beam by using the same technique as for the free vibration tests. Resonance was obtained by adjusting the driver frequency to obtain maximum displacement of the beam. At this time the resonance bandwidth frequency was measured by adjusting the driving frequency until an amplitude of about 0.707 of the resonance amplitude was obtained. This occurred at two frequencies, one above resonance, and one below resonance. The supports were then repositioned and the second mode frequency was obtained using the same procedure.

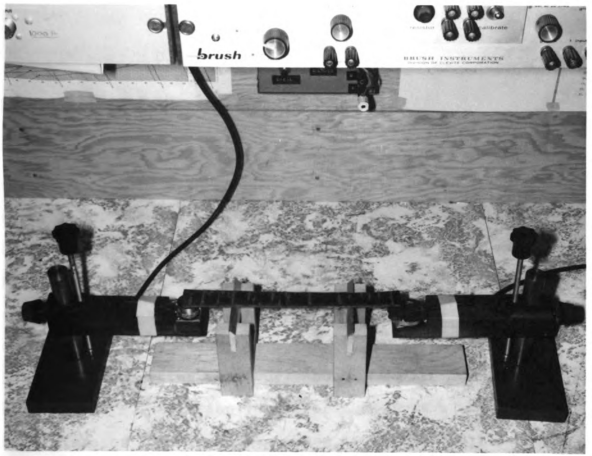

Figure 10.--Bark specimen supported at the nodal points for forced vibration tests.

DISCUSSION OF RESULTS

Effectiveness of the Testing Chamber

Mechanical properties of fiberous and woody materials usually vary more with changes in moisture content than temperature. Decreases in either temperature or moisture content tend to increase strength and elasticity, however, changes with moisture content are much larger. For example, wood changes in strength and elasticity about 5 per cent for a one per cent change in moisture content. However, these same properties only vary about one-half per cent for a degree F. variation in temperature from a base temperature of 70 degrees F. (Wood Handbook, 1955). Thus to measure the mechanical properties of bark and green wood effectively both the temperatures and moisture contents that the specimen had while still on the tree should be maintained. Thus the function of the chamber was to maintain a constant normal room temperature and keep humidity as high as possible.

During the tests the chamber temperature could be regulated successfully between 69 to 73 degrees F. However, the humidity could not be raised over 75 per cent

without causing frost formation on the air conditioner. Under these conditions 10 to 15 per cent of the moisture content in the bark specimens was lost in a two hour period. To reduce this effect to a minimum specimens were tested immediately upon being brought from the field. Testing time for an individual specimen was about one-half hour. It is assumed that what moisture loss took place during collection and testing increased the strength and elasticity of the bark specimens, but it is not known to what extent. Wood specimens tested had moisture contents of about 38 per cent which is well above the fiber saturation point of 30 per cent. It has been reported (Wood Handbook, 1955) that wood strength does not begin to increase until the fiber saturation point is reached. On this basis what moisture loss that occurred in the wood during testing was probably not significant.

As a result of the above experience it is evident that humidity should be kept as high as possible to reduce such moisture loss. Certainly rapid testing is necessary. A better method may be to construct a small chamber of Plexiglas around the test fixture. Then high humidities could be maintained without adverse effects to the cooling system and electronic equipment kept from high humidity. It must be emphasized that bark tissue is primarily a living tissue and life processes will stop soon after collection unless additional moisture is supplied. Therefore an

environment of 100 per cent humidity will not eliminate the change in mechanical properties.

It may be profitable to study the effect of storage in high humidity and water environments at various temperatures on bark tissues for selected time intervals after collection to see how mechanical properties change. The use of the non-destructive vibration tests used in this study would be very suitable for this purpose. This type of information may also be of considerable use in estimating the change in properties which takes place over the time interval from collection until the test is completed.

Physical Structure of Bark Tissue

In an attempt to study the structure and composition of bark tissues a transverse section was made of living tissue using a freezing microtome. Because of the vast difference in texture between the phloem and periderm it was not possible to make a section less than 30 microns without crushing the phloem tissue. The resulting section did not show as much detail as desired owing to low light transmissivity. However, with the aid of additional observations with a compound microscope and the use of some standard references (Esau, 1964; and Schneider, 1945) a classification of the tissue on the basis of location and probable structure was made.

As illustrated in Figure 11 the bark was divided into four major radial layers of tissues for the purpose of this study. Starting with the functioning phloem at the interior and proceeding in an outward radial direction tissues appear to gradually decrease in percentage of living cells. The extreme outer tissue, the scale periderm, is almost completely composed of non-living cells. Bark tissues tested were found to have moisture contents of 110 to 145 per cent which is a general indication of a large percentage of living cells in an average cross section. This is because the living cells contribute a large amount of free moisture to tissue in the form of the cytoplasmic fluid which is about 95 per cent water.

The functioning phloem composed about 10 per cent of the thickness of the section. It is shown at the top of the figure as composed of alternating rows of ray parenchyma as dark bands and sieve cells. The ray parenchyma rays were about six to eight cells wide and can be seen to extend deep into the nonfunctioning phloem. The browning of these cell walls was caused by exposure to air after sectioning. The hollow sieve cells are the food conducting elements in the bark and are shown as white dots between the ray parenchyma. The long axis of the sieve cells is in the longitudinal direction and the long axis of the ray parenchyma is in the radial direction. All cells in functioning phloem are living and characteristically have only primary walls.

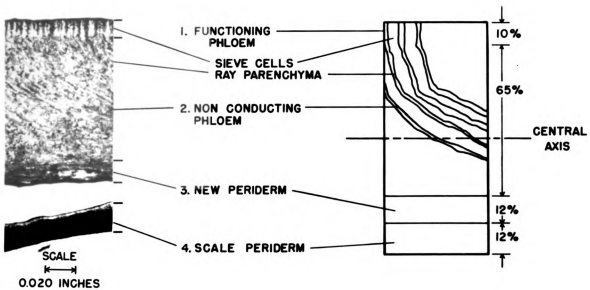

Figure 11.--Transverse bark section showing location and relative thickness of the major tissue regions.

The major portion of the bark is composed of the nonfunctioning phloem region. This tissue is accumulated from layers of functioning phloem of preceding years which ceases to function at the end of the growing season. A considerable amount of consolidation and collapsing of the old tissue takes place as evidenced by the increasing slope of the ray parenchyma with respect to the radial direction. For example in the nonfunctioning phloem, the rays are oriented at an angle of about 45 degrees to the radial axis. This indicates that deformation of at least half the original thickness has taken place over a period of years. Under this loading many of the sieve cells eventually collapse and parenchyma cells enlarge and fill the void, (Esau, 1960). In a related study of Sweet Cherry (Prunus arium) phloem, Schneider (1945) found that secondary fibers develop between the rays and intermingle between the conducting tissue of the preceding year. He observed the cells between the rays were a combination of partially collapsed sieve cells, fibers, cavities and parenchyma cells. This appears to be the case also with the specimen under study. Large fissures are also found along the rays as observed by Schneider. Therefore it is assumed that the living cells in this tissue are composed of ray parenchyma between the rays. The sieve cells and fibers are essentially nonliving. The general appearance of this tissue is soft and fibrous with a spongelike

response when pressed in the radial direction. This helps the bark cushion and protect the functioning phloem.

The outer 25 per cent of the bark is composed of two periderm tissues, the new periderm and an outer scale periderm. In general, the major function of this tissue is to regulate the rate of gaseous exchange and to prevent moisture loss. To form this type of moisture barrier periderm cells are tightly packed and have walls formed from layers of suberins and waxes. Under the light microscope the tightly packed nature of these cells was observed. This is shown in Figure 11 by the dark areas. During collection of the specimens, July 8, 1965, the outer periderm was loosely attached to the bark section. Its removal exposed a living periderm, green in color, underneath. In mature periderms, the walls become layered with waxes and the cells become isolated from the living tissue and die. It is assumed that this is the case for the scale periderm in this section, with the exception of a few layers of cells on the inner surface which may have been living since they browned some after detachment. After oven drying the scale periderm did not become stiff and brittle as did the other bark tissues but retained much of its original flexibility. This could be explained by the waxy structure of the cell walls. The other tissues having pectic and other compounds in the walls stiffened with drying. However, in the periderm, the cellulose mesh

of the primary cell walls is filled with wax and suberin. Suberin and wax are both fatty substances. Because of their chemical nature these substances did not become hardened from the oven drying.

Under closer examination, it appeared that the periderm cells had their long axis in the tangential direction. In woody tissue maximum strength lies in the direction of the long axes of the cells. Therefore it is probable that the maximum strength of the periderm is in the tangential direction.

Strength of Bark

As a further step in the preliminary investigations the maximum tensile strength and maximum cambium shear strength of bark were studied. The purpose of these tests was to obtain some initial information about the response of the material under load and to compare this information to data reported by Adrian and Fridley (1963) and Brown (1965).

Mechanical strength of bark.--For the maximum strength tests specimens were cut into necked sections as shown in Figure 12 and subjected to tensile loadings at a constant strain rate. In all tests performed failure occurred in the necked section. Stresses were calculated on the basis of the unloaded area of the necked cross section.

A typical failure curve for a longitudinal bark section is shown in Figure 13. As loading is increased

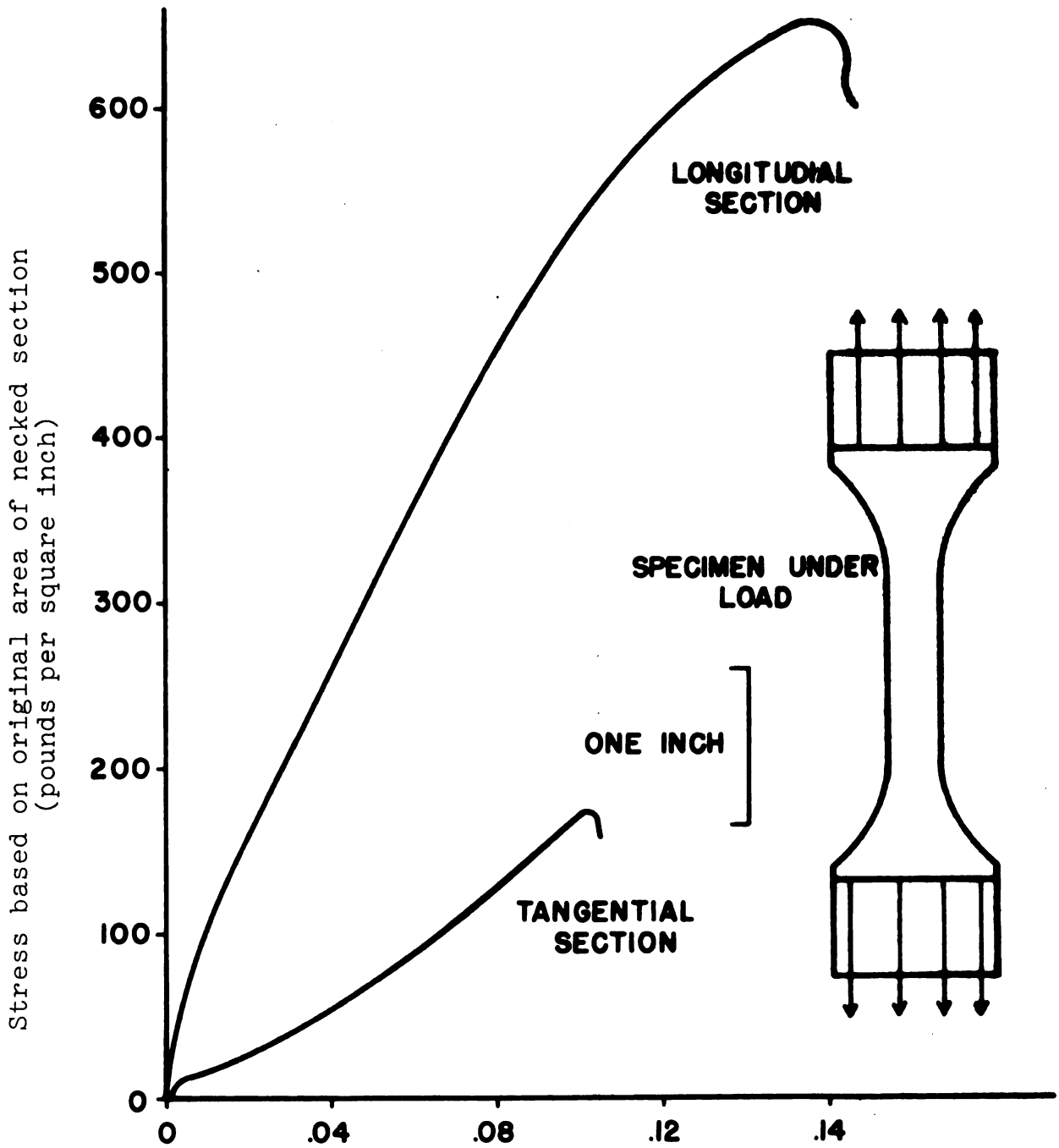

Figure 12.--Failure of a longitudinal bark specimen subjected to tensile loading.

the curve becomes more non-linear until failure of the specimen. The initial non-linear portion of the curve is presumed to be due to some stress relaxation of the bark under load. In the final stages of loading the slope of the curve decreases more rapidly. During this phase actual failure is taking place by incremental failure of fibers and tissues accompanied by sliding and continued failure in the tissue. This is also evident from the jagged failure surface as shown in Figure 13. The new periderm failed in a smooth surface presumably along the cell boundaries. If an outer scale periderm was present it usually failed about one-half the total elongation. The maximum displacements at failure are not particularly meaningful for this type of cross section except for comparison to failure of tissues at other orientations or failures of the periderm The displacements were corrected for deflections of the load cell relief spring and an attempt was made to determine if slip had occurred under load. It is obvious that any slip while loading could have a large influence on any loading curve. Two visual observations were made, one by observing movement of a line made on the specimen at the edge of the clamp before loading and secondly by observing the condition of the clamped surface after failure had occurred. Some slight movement with respect to the lime on the specimen took place during loading. However it is difficult to determine whether this was due

Figure 13.--Failure of a longitudinal bark specimen subjected to tensile loading.

to some slight slip or non recoverable strain produced during loading. Examination of the clamp surface revealed distinct impressions of the serrated surface of the clamp indicating slip had not occurred. In the longitudinal direction the strength of the periderm is about 1.5 times that of the bark. However, the periderm fails before the bark. Thus the periderm contributes some initial strength to the bark but soon fails and contributes no strength when the bark reaches the rupture point.

Tangential sections loaded in the same manner failed at much lower stresses. From the smooth failure surface it is suspected that failure occurred mainly along the cell boundaries as shown in Figure 14. This is because in the longitudinal sections cells had their long axis in the longitudinal direction. However in tangential sections the force was applied at a right angle to the long axis of the cell. Further there is no known reason to suspect that the cell wall strength is less in the direction of its short axis than in the direction of its long axis. Therefore the difference in failure strength must be attributed to failure of cell boundaries rather than the cell wall itself. If the above argument is true the strengths listed in Table 2 are comparisons of longitudinal rupture strength to tangential cell boundary strength, the former being about nine times greater.

Figure 14.--Failure of a tangential bark specimen subjected to tensile loading.

The failure curve for the tangential section was initially curved upward. This type of response indicates a material which increases in stiffness as deformation increases. It is proposed that this is not the case and the response can be explained on the basis of the physical structure of the material. In the natural state tangential sections are on an arc about the tree limb. Therefore when first loaded, the specimens first go through a period of reorientation and realignment in the direction of the applied force. When a higher level of stress is reached the cells must also start to deform physically. Normally deformation of the cellular tissue should produce a stress curve of decreasing slope. It is thought that a combination or reorientation and deformation accounts for the linear appearance of the last part of the failure curve.

Failure stresses are in a ratio of about nine to one. Adrian and Fridley (1963) reported a ratio of about four to one for prune trees. However, there is little basis of comparison owing to the difference of species and possibly moisture content.

Since the scale periderm was readily detachable it was tested separately in longitudinal and tangential directions. The directional strength properties of this tissue were opposite to that of the bark tested in the preceding section. In these tests clear specimens without cracks or lenticels were selected. Longitudinal sections

TABLE 2.--Ultimate stress and elongation for necked bark sections under tensile loading. R = 1.5 inches per minute.

Sample Number	Tensile Stress (psi.)	Elongation (inches)	Thickness (inches)
	Longitudinal Section		
L1	820	-	.155
L2	678	.151	.158
L3	494	.146	.125
L4	730	.212	.363
L5	563	.181	.358
Average stress	657 psi		
	Tangential Section		
T1	124	.120	.165
T2	82.7	.108	.150
T3	58.2	.104	.125
T4	44.6	.114	.230
T5	42.3	.113	.190
Average stress	70.4 psi		

failed soon after loading along smooth horizontal failure planes. It is suggested that failure took place along the cell boundaries. From a microscopic examination of the section in Figure 11 it appeared that the long axis of the periderm cells was in the tangential direction. If this is true, the highest strength of the periderm should be in the tangential direction by a similar argument as presented for the bark. In fact tensile strength in the tangential direction was about three times that of the longitudinal direction. The tangential sections had a non-linear loading curve similar to that for bark in longitudinal sections. However the periderm tissue did not fail upon reaching the maximum strength but was then capable of large plastic deformations at the same level of applied force. During cross extension of the area the plastic section became considerably less. This means that the true stress at rupture was much larger than that calculated on the basis of the original area. From this behavior under loading some theories of reaction at the cellular level are advanced. The initial part of the curve up to the plastic region is typically nonlinear owing to stress relaxation under small deformation. When the "yield stress" is reached plastic flow takes place over larger deformations. These cells are dead with thin walls encrusted with waxes which possibly act as a lubricant and allow for some slipping between the cells during large deformation of the cells.

TABLE 3.--Ultimate stress of periderm sections under tensile loading. R = 1.5 inches per minute.

Longitudinal Sections			Tangential Sections		
Sample Number	Stress (psi)	Thickness (inches)	Sample Number	Stress (psi)	Thickness (inches)
L6	1240	.023	T6	3520	.018
L7	1058	.0223	T7	3430	.020
L8	1035	.020	T8	2780	.020
L9	845	.020			
L10	615	.021			
Average	958.6 psi		Average	3243.3 psi	

In general the periderm elongations were as much as one inch or about 40 per cent of the original length. Thus from Table 3 it is evident in the longitudinal direction that the periderm is capable of extensions up to 5 times greater than the bark extension before rupturing.

If the elastic modulus of the periderm and the bark were the same in the tangential direction, on the basis of the relative thickness, the periderm would support about 1/20 of the total force. They would of course have the same stress. However, since the periderm is capable of supporting at least 5 times as much stress as the bark, the periderm may support one-fourth or more of the total

load. In addition, since the periderm is capable of greater extensions, it serves to help resist rupture of the bark in the tangential direction. Therefore, when the bark and periderm are subjected to large tangential elongations, such as produced in torsion, it would be possible for the bark underneath the periderm to rupture, but give no visible evidence of rupture, since the outer periderm would still be intact.

Longitudinal cambium shear strength.--In these tests the specimens of bark and green wood were prepared and loaded as shown in Figure 7. In preparing the samples an attempt was made to minimize the effect of moments acting at right angles to the shear plane by cutting the wood to the same thickness as the bark. The effect of a moment would lower the value of the calculated shear force. It must also be assumed that some misalignment and prestressing occurred while clamping the specimen. The average shear stress for Montmorency cherry bark as determined by this test was the average of the stresses listed in Table 4. This test might be improved by supporting the clamps by knife edges to correct alignment during loading. This data could not be compared to that of Brown (1965) since he used a normal (radial) pressure on the section when measuring shear stress.

TABLE 4.--Maximum longitudinal cambium shear strength.

Shear Stress (psi.)
33.5
27.8
30.5
31.8
25.7
35.7
27.1
27.9
26.1
Average stress 29.6 psi

Elastic and Viscoelastic Response of Bark and Green Wood to Frequency of the Applied Stress

All specimens tested including the aluminum showed some viscoelastic behavior. All materials with the exception of aluminum exhibited a detectable stress relaxation and all demonstrated a change in the complex modulus of elasticity with changes in frequency of the applied stress.

Static Tests.--In these tests all materials tested were supported as simple beams and center loaded at a constant rate of deformation. The bending stress-displacement relation for all materials was visibly non-linear with the exception of the aluminum. The amount of non-linearity of the relation depended on the amount of damping in the material. Bark for example, had the largest amount of curvature and in later tests bark was also found to have the largest

value of the dimensionless damping ratio η'. A typical loading curve for bark is shown in Figure 15. Values of stress were calculated from experimental data using equation 1. An equation to represent this type of loading behavior has been proposed previously by Ferry (1960) and was presented as equation 3 in this Thesis. In this equation the amount of stress at any time t is reduced by an amount exp $(-tH(\tau)/\eta)$ where $H(\tau)$ is related to the elasticity of material and η is the damping constant in pound (second)^2 per square inch. Thus for larger values of η the curvature of the stress curve becomes more pronounced as time increases. No attempt was made to determine values of η from the loading curves. To do this would also require determination of $H(\tau)$ for various values of strain rates, R. Experiments of this type are reserved for future research. However, equation 1 was used indirectly in calculating the relaxation modulus E(t) and extending the loading curve as shown in Figure 15 using equations 3 and 4 as proposed by Ferry (1960) and Chang (1964). By use of equation 4 a frequency f was calculated for the storage modulus. For example f for the tangent modulus (relaxation modulus, E(t); storage modulus, E'(1/t))in Figure 15 was calculated by the relation $t = 1/2\pi t$ cycles per second. Values of the secant modulus (tangent modulus) were calculated using equation 2. These moduli are listed later in this section in Tables 5 and 7 and are discussed in comparison with

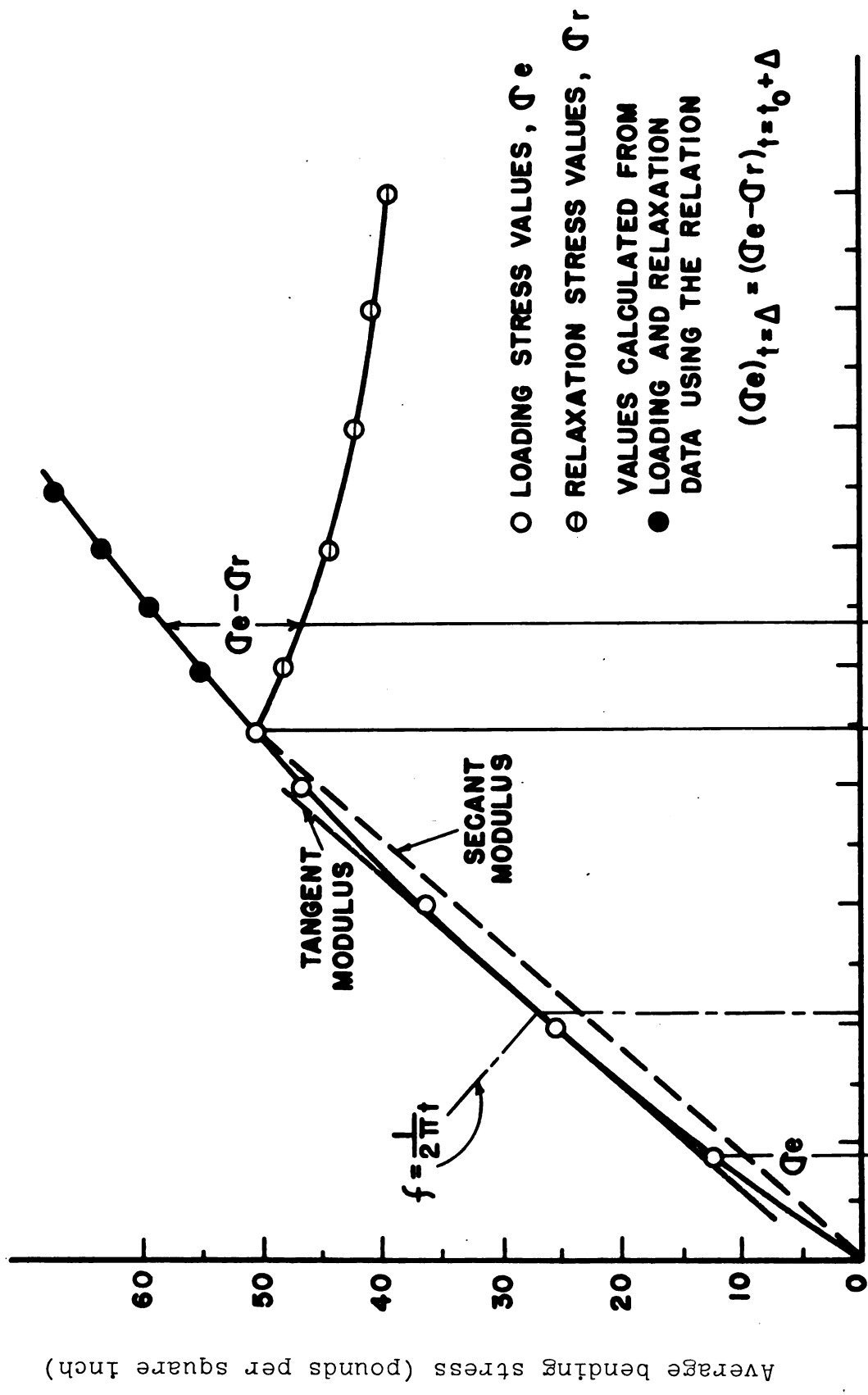

Figure 15.--Loading and relaxation of bending stresses for bark specimen B5.

moduli obtained at higher frequencies of applied stress. By use of the equation $(\sigma_e)_{t=\Delta} = (\sigma_e - \sigma_r)_{t = to + \Delta}$ suggested by Chang (1964), the loading curve for bark shown in Figure 15 was extended from the loading and relaxation data. In this relation σ_e and σ_r are the loading and relaxation stresses respectively at times Δ and to + Δ respectively.

Stress relaxation curves for representative samples of the materials tested in this section are shown in Figure 16. Again the amount of non-linearity in these curves depended on the amount of viscosity in the material represented by the damping constant η. The relation between η and the relaxation stress, σ_r, in a material loaded at a constant rate of elongation R to time t_o was proposed by Chang (1964). This relation is

$$\sigma_r = R \int \eta H(\tau) \exp(-t/\tau)[\exp(t_o/\tau - 1] \qquad (44)$$

where τ is defined as the ratio of the damping constant η to the elastic spectrum $H(\tau)$. In this relation the term exp $(-t/\tau)$ again accounts for changes in stress depending on the value of η and t.

This means that for the same amount of stress applied in extension the bark has the ability to relax under load at a higher rate than the wood. This is an indication that the bark could undergo larger deformations than wood before rupturing. In the actual bending of a tree limb for example, both the outer wood fibers and the bark undergo

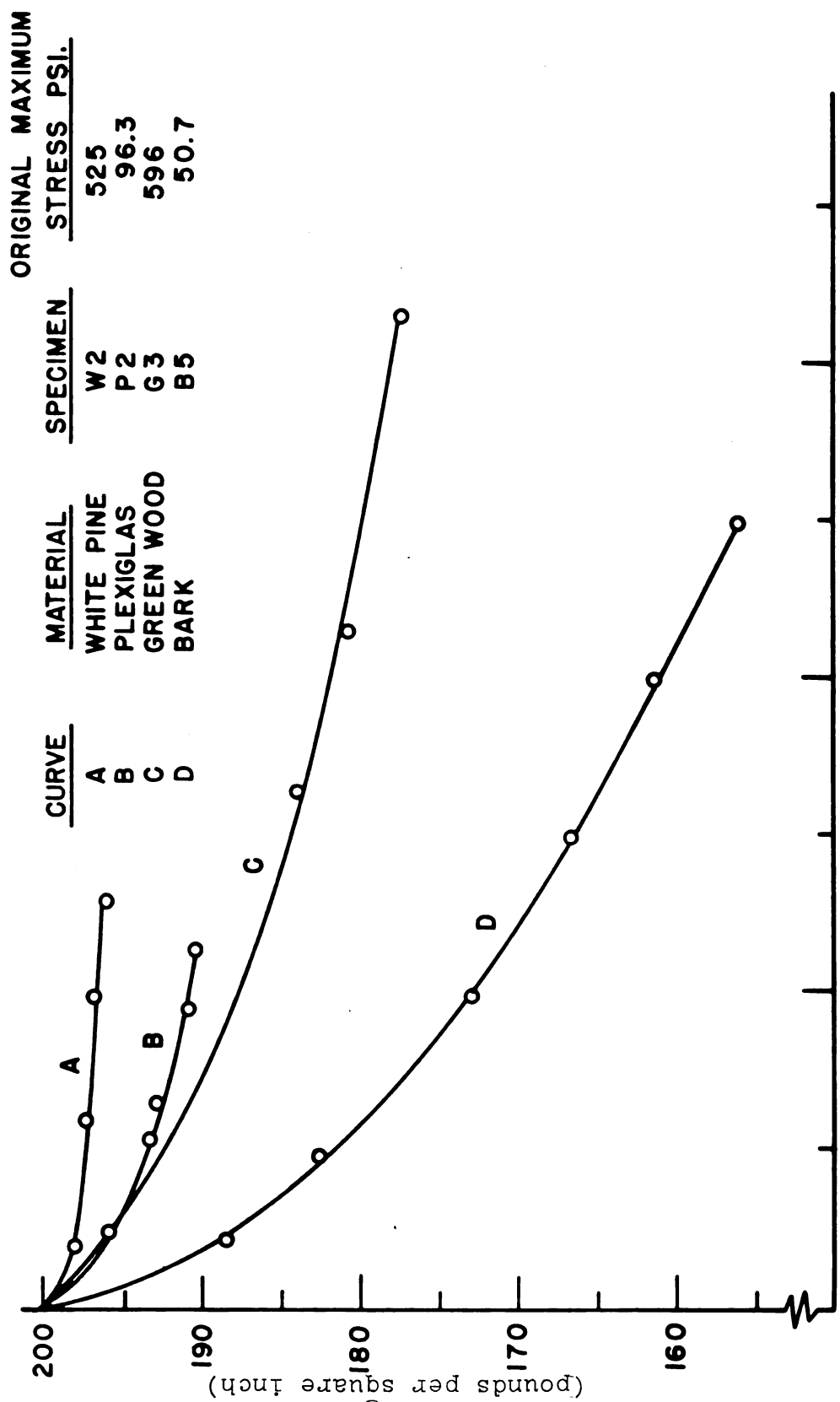

Figure 16.--Primary relaxation of bending stresses reduced to the same initial values for some materials tested.

essentially the same elongation. If both the bark and wood had the same elastic modulus similar stresses would be produced in both tissues and the above argument would apply to failure. However, since the elastic modulus of bark is only about 1/50 of that of wood, it means that the bark is stressed only 1/50 of the amount of wood for the same elongation. Thus in all probability in simple bending the wood would fail first. Bark injury would occur as a result of the clamp slipping in the longitudinal direction. This is a result of the stiffness ratio between the bark and wood. Failure in this case results from large elongations being applied to the bark. The wood being much stiffer resists being elongated and shear failure occurs at the cambium layer.

Sonic tests.--Of the two testing techniques used, the free vibration technique using cantilever beam geometry was superior to the forced vibration method. The free vibration method was simpler, required the least amount of instrumentation and produced the most consistent results. The logarithmic decrement Δ and the damping ratio η' were calculated from data obtained from the wave form in Figure 17. The decay of successive amplitudes of this wave as plotted in Figure 18 gives a curve whose slope is equal to the logarithmic decrement.

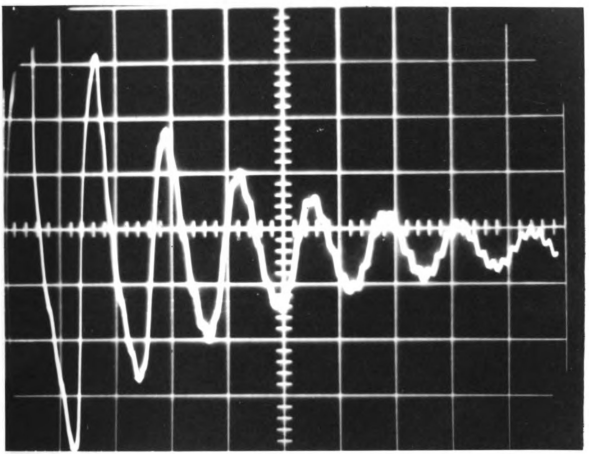

Figure 17.--Damped oscillations at the free end of a cantilever bark specimen.

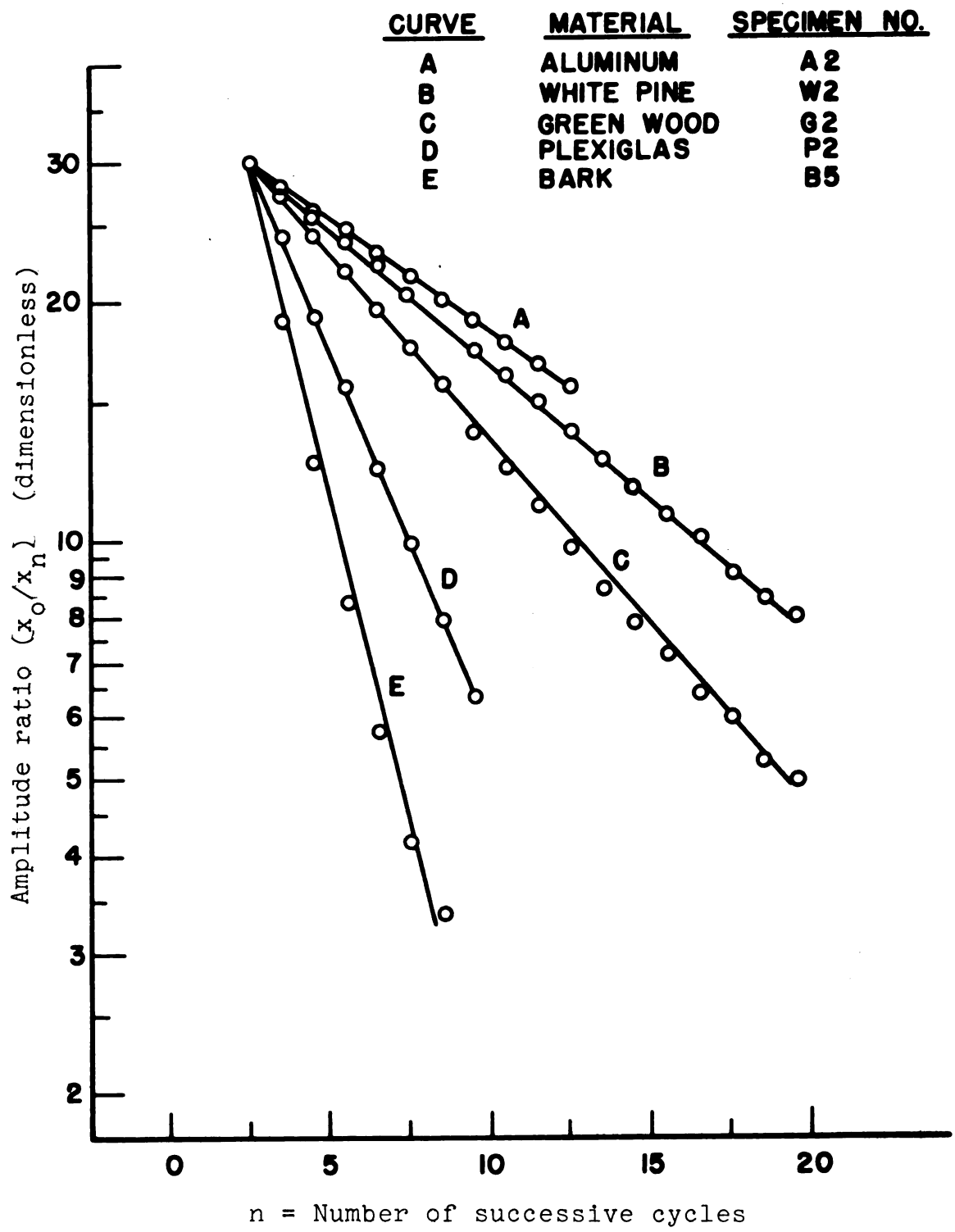

Figure 18.--Aplitude reduction of successive cycles at the free end of cantilever specimens.

Values of η' were calculated using the approximate relation $\eta' = \frac{\Delta}{2\pi}$. It was not necessary to use equation 40 since η' was small. The highest value of η' was only 0.084. From Figures 3 and 4 and Table 1 in the Appendix it is evident that the error resulting from using this approximation is negligible. A least squares linear curve fitting technique in fitting a straight line to the data was not used since it was not felt this would add significantly to the accuracy of the experiment. All bark specimens tested using this technique had nearly the same values of Δ which is shown indirectly by the calculated values of η' in Table 5. Of course the use of the logarithmic decrement assumes an exponential decay of amplitude. This is shown to be a good approximation for most materials tested. The green wood and to a greater extent the bark showed some curvature in the logarithmic decrement curve. This error becomes serious for high values of damping and requires the use of approximation procedures as described in the Theoretical Analysis section of this Thesis. Frequencies for these tests ranged from 7.6 to 117 cps depending on the material. Notice the curves for materials in Figures 16 and 18 fall in the same order. Both these sets of curves are measures of internal damping in the material. Steeper slopes correspond to a relatively higher energy loss per cycle in the material. For a meaningful comparison the values in Figure 16 whould be compared only

to initial slope values in Figure 18, thus using a similar value of experimental time. Notice after one second the relaxation rate of Plexiglas has reduced sufficiently to approach that of green wood.

The forced vibration tests were originally intended as a check on the other methods, however, this test was also useful in obtaining information at higher frequencies of applied stress. In these tests a sub-harmonic resonance of order 4 of the first mode was found to exist in the specimens for a driving frequency of half the first mode frequency. This was an aid in correctly determining the first mode frequency since the period of the sub-harmonic wave was easily recognized being twice that of the driving wave as shown in Figures 19 and 20. The forced vibration method has the added advantage of determining the behavior of the material at still higher frequencies by using higher modes, (Figure 21). However, in practice modes higher than the third were difficult to detect since the resonance amplitude decreased for each higher mode and resonance could not be separated easily from the background noise present in the system. The only satisfactory third mode resonance obtained for the materials tested was for one of the white pine specimens at 1357 cycles per second as shown in Figure 21. This was also the only case in

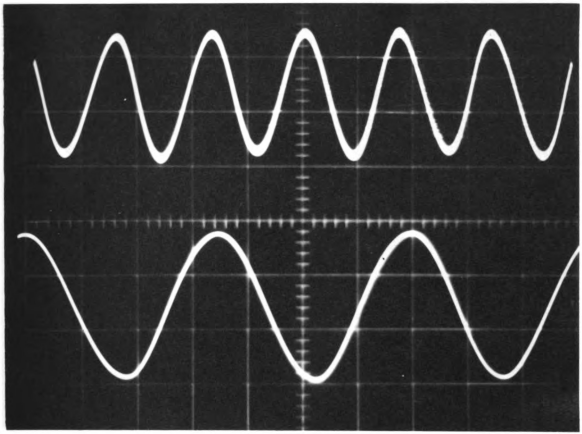

Figure 19.--Forced vibration of a simply supported specimen showing: top, driving wave at half the first mode frequency; bottom, resulting oscillation of the beam (fourth order subharmonic of the first mode frequency).

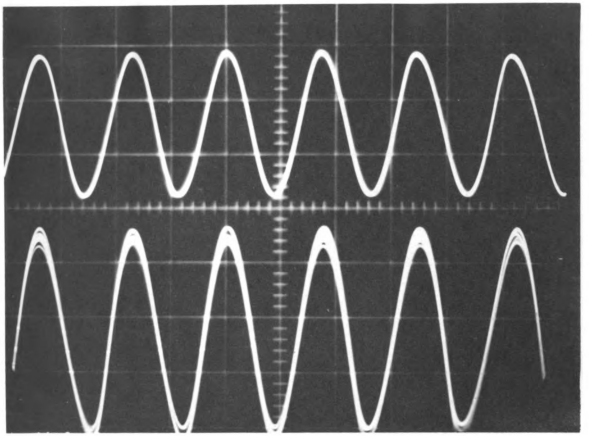

Figure 20.--Forced vibration resonance at the first mode for a simply supported specimen showing: top, driving wave; bottom, resultant vibration of beam.

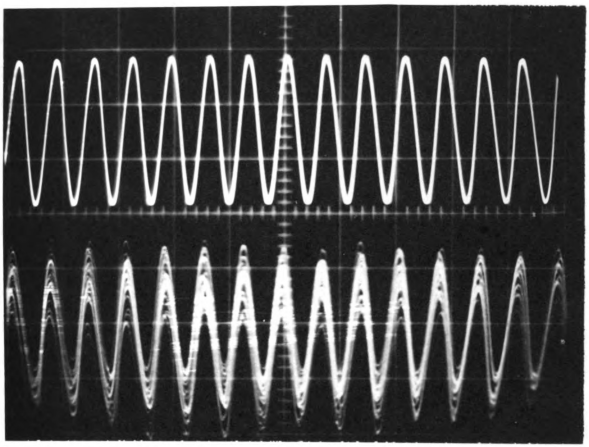

Figure 21.--Forced vibration resonance for the third mode showing: top, driving wage; bottom, resultant vibration of beam.

which it was necessary to apply the Goens' correction factor T_n. In this case the value of E was adjusted by multiplication with a value of T of 1.0154 calculated from equation 12. It is also possible to change resonance frequencies for the same specimen in both free vibration and forced vibration tests by altering the physical dimensions of the beam.

Some difficulty was encountered in using the forced vibration method with specimens of low stiffness such as bark and specimens of high stiffness such as aluminum. Except for two bark specimens, B3 and B4, which were thicker than the others and consequently had a higher resonance frequency the first mode of the bark specimens was below the lower frequency limit of the oscillator. This was not realized at the time of testing and erroneous values of the elastic modulus were calculated which were about twice the correct value. However, since all modal frequencies are related by fixed constants which may be calculated from elastic theory by assuming a more probable value of E the first two modal frequencies were calculated. Upon comparison with the erroneous data it was apparent that the sub-harmonics of the second mode was mistakenly used for the first mode frequency. This points out a serious danger in this type of testing of incorrectly selecting the wrong mode or a sub-harmonic for the correct

modal frequency. Since the modulus is a function of the square of the frequency this can lead to large errors. If the approximate value of the elastic modulus is known, the approximate value of the modal frequency can be calculated before testing.

However if the modulus changes rapidly over a few decades of frequency such as in the bark tissue, this technique is not as helpful. With the aluminum samples a difficulty of a different nature was encountered. Due to the high stiffness of these beams the power required to excite resonance was near the power limitations of the driver. However, this method was very suitable for the other materials tested which were in the intermediate stiffness range such as green wood, white pine, and Plexiglas specimens.

Values of the damping ratio η' were calculated using the frequency bandwidth of the resonance curve and equation 23. This method was not found to be highly accurate since measurements must be made by visual reference on an oscilloscope screen. Also it was somewhat difficult to adjust the oscillator to the exact frequency to determine the sideband resonance points. Materials having relatively high damping such as the bark had a wide bandwidth extending over 10 to 15 cps. Materials with lower damping such as the white pine had a narrow bandwidth of two to three cps. Since η' is directly proportional

to the square of the bandwidth, the chance for error increases greatly for materials having a narrow band width. Therefore values of η' listed in Table 5 for forced vibrations are not to be considered highly accurate for aluminum and white pine.

Some of the common engineering constants determined as a result of this investigation for the materials tested are listed in Table 5. Notice that the values of Young's modulus of elasticity are not constant but become larger with increases in frequency of the applied stress. Values of the elastic modulus for some engineering materials such as concrete and wood were obtained previously, but only for a fixed frequency. In these references the value obtained was called the sonic modulus. However, these authors apparently did not recognize that due to the presence of some viscoelastic effect in all these materials that the modulus actually varies with frequency as shown in Table 5. Values of elastic modulus in this table are in fact only estimates of the true complex modulus E^* which is equal to $E_1 + iE_2$. Thus only in cases of wood and aluminum where E_2 is small are these values approximately correct. The modulus of elasticity for bark found in these tests was very low compared to green wood and ranged from about 10,000 to 40,000 psi. over the frequency range used. Modulus of elasticity of green wood ranged from about 500,000 to 700,000 psi.

TABLE 5.--Youngs' modulus of elasticity and damping ratio for bark and some other materials tested for different frequencies of applied stress.

	Specimen	Density lb/ft^3	Quasi-Static rate = .05 ipm. Loading Time sec.	Quasi-Static rate = .05 ipm. Secant Modulus psi.	Free Vibration Frequency f cps.	Free Vibration Elastic Modulus E psi.	Free Vibration Damping Ratio n' Dimensionless	Forced Vibration Frequency f cps.	Forced Vibration Elastic Modulus E psi.	Forced Vibration Damping Ratio n' Dimensionless
BARK TISSUE (Montmorency Cherry)	B1	78.9	250	12,050	7.6	32,030	.075	+	+	+
	B2	73.2	242	11.630	5.8	35,370	.084	+	+	+
	B3	74.2	215	12,210	7.5	37,914	.060	34	42,920	.042
								93	42,050	+
	B4	70.7	223	9,234	8.35	29,930	.061	29	31,970	.085
								83	34,780	+
	B5	68.8		21,720	6.45	39,890	.080	+	+	+
GREEN WOOD (Montmorency Cherry)	G1	38.4	132	466.900	58.4	493,830	.015	276	658,300	.019
	G2	35.6	160	525,800	62.5	572,640	.017	290	740,840	.017
PLEXIGLAS	P1	75.0	61	422,900	45.5	578,600	.039	205	693,400	.021
	P2	75.0	63	415,000	45.8	597,600	.041	209	734,200	.024
WHITE PINE	W1	26.0	67	1,074,000	113.5	1,168,000	.009	490	1,135,000	n.m.
	W2	25.4	62	1,143,000	115	1,166,000	.013	501	1,338,000	n.m.
								1357	1,345,000**	*
	W3	24.6	65	1,164,000	n.m.	n.m.	n.m.	503	1,311,000	n.m.
ALUMINUM (alloy)	A1	168.0	32	9,298,000	n.m.	n.m.	n.m.	n.m.	n.m.	n.m.
	A2	168.0	22	9,160,000	119.5	9,482,000	.0099	556	9,481,000	*

n.a. - not applicable
n.m. - not measured
\+ - fundamental resonance below frequency response of oscillator
* - exceeded power limits of driver
** - corrected for shear and rotation inertia

over a similar range of frequencies. However, as a result of the large increase of the elastic modulus for bark as compared to the green wood in this frequency range the stiffness ratio between bark and wood decreases from about 50 to one at quasi-static conditions to about 15 to one at frequencies between 100 to 200 cycles per second. The behavior of these materials is discussed in detail in the next section using the more applicable theories of viscoelasticity. However, it is apparent that owing to the much higher stiffness of wood as compared to the bark that the properties of the wood largely determine the response of the limb to applied stresses. When a shaker clamp is attached to the limb the bark is compressed between two media which are much stiffer than the bark. Reduction in bruising would of course result from using a shaker pad which has less stiffness than the bark. The internal damping of bark was about five times higher than that of green wood. This ratio remained at about the same value for the two comparisons made at different frequencies for the free and the forced vibration tests. Thus in free vibration the bark has a damping effect on free vibrations of the limb. Since the bark is at the maximum distance from the neutral axis a thin layer of bark is in a position where it can produce the maximum possible damping effect.

The elastic parameters discussed above for bark and green wood can not be compared to existing values since they are not available in literature. However, comparisons may be made for the secant modulus (Youngs' modulus) of the other materials to existing published values. These values are averages and dependent on the exact structure and composition of the individual material. Values used for this comparison were Plexiglas- 400,000 to 600,000 pounds per square inch (Hodgman, 1952), white pine - 1,170,000 pounds per square inch (USDA Wood Handbook, 1955), and aluminum - 9.3 - 10.6 x 10.6 pounds per square inch, (Baumeister, 1958). Values of Plexiglas are given as a range of values since the slope of the stress-strain curve changes during loading; values of aluminum are variable depending on the per cent of alloys present. These values compare very well with those obtained in Table 5 with the exception of the aluminum for which a value of about 9,200,000 was obtained for Youngs' modulus. Since the composition of these aluminum specimens was unknown, an additional beam of 6061-T6 aluminum was tested. Using the test equipment a value for the elastic modulus of 10,040,000 was obtained which is the correct value for this material. As a result of this it was suspected that the low value for the other aluminum beams was due to differences in composition and residual stresses resulting from machining.

The density of bark was quite high and showed a large variation from 68 to 78 pounds per cubic foot. Bark was about twice as heavy as green wood. However, after drying several weeks in an oven bark densities stabilized at 31 to 32 pounds per cubic foot based on the original dimensions. The close agreement in dry densities suggests that the variation in wet densities was due to differences in moisture content and not differences in structural density of the bark. It is of interest to find the same structural density in these bark specimens since they were collected at random from several different cherry trees. The thickness of bark ranged from .098 to .161 inches. Since in cherry bark the old phloem from the preceding year is not severely crushed but becomes part of the non functioning phloem and the outer periderm scales off yearly, increases in thickness are directly related to the age of the bark. The resulting indication is that mechanical properties of cherry bark would not be expected to have much dependence on age. In fact no effect of thickness was apparent on values of Youngs' modulus for bark. Dry weight density of the green cherry wood stabilized at about 26 pounds per cubic foot. The differences of dry weight densities in bark and wood is explained on the basis of the large amount of hollow conducting cells in wood as compared to a high percentage of smaller living cells in the bark having cellular conclusions.

Viscoelastic considerations.--At best theory of elasticity can only be used to calculate general trends in material constants but cannot be used effectively to explain behavior of materials which are highly viscoelastic. For this reason the data in Table 5 is recalculated in terms of viscoelastic components and presented in Table 7 and Figure 22. In this manner it was possible to separate and examine separately elastic and viscous effects by the use of the components of the complex modulus; $E'(\omega)$, the storage modulus and $E''(\omega)$, the loss modulus. From the use of the relation $E'(\omega) \approx E(1/t)$ described earlier, values of the storage modulus were calculated for very low frequencies using the "static" loading data. These values are listed in the third column of Table 7 and shown in Figure 22. These values are significantly lower than values obtained at higher frequencies particularly for bark.

Plexiglas was the only one of the three check materials used in this test whose viscoelastic properties over a wide range of frequencies was known. For this reason a detailed comparison of results of this study are made before discussing the behavior of the other materials. Mechanically, Plexiglas is classed as an uncross-linked amorphous polymer. Physically this means that Plexiglas does not display instantaneous elasticity on loading and that $E(t)$ tends to zero for large values of time. Ferry (1960) describes this material as responding to external

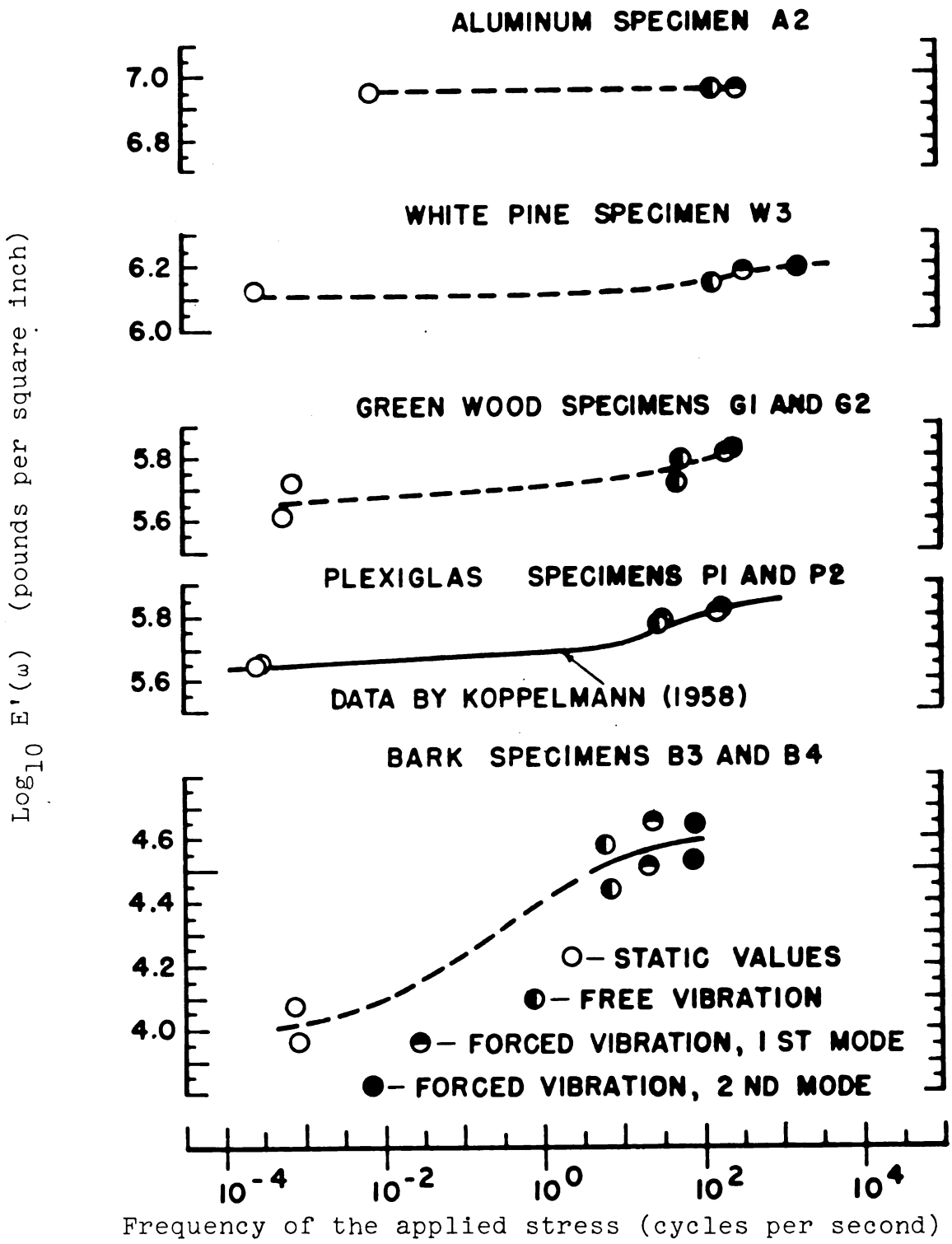

Figure 22.--Storage modulus for some of the materials tested plotted logarithmically against frequency of the applied stress.

stress by local adjustments at the molecular level through entanglement connections between the molecules. As shown in Figure 22 the storage modulus for Plexiglas increases gradually an amount about 50 per cent of its original value over about five decades of frequency. Since E(t) is nearly the mirror image of the storage modulus one would therefore expect the relaxation modulus to decrease slowly over several decades of time. This is in fact shown to be the case in relaxation curves presented by Ferry for Plexiglas. Fortunately a rather complete set of dynamic data by Koppelmann (1958) was available to compare to data obtained in this study. Koppelmann used a non-resonant technique of testing in obtaining this data as described in the Related Literature section of this Thesis. Values of $E'(\omega)$ for Plexiglas as shown in Figure 22 are in very good agreement with those by Koppelmann. Note that this material has a distinct inflection point in the storage modulus curve near 10 cycles per second. Koppelmann found that the loss tangent of this material increases gradually from low values of about .045 at both ends of the frequency spectrum to a maximum value of about .10 at 45 cycles per second. These values are compared with those found in this experiment in Table 6.

TABLE 6.--Comparison of experimental values of loss tangent for Plexiglas with those by Koppelmann (1958).

	frequency (cps)			
	10^{-3}	45	200	10^{3}
Koppelmann	.038	.10	.065	.048
Experimental Values	-	.077-.082	.060-.068	

Ferry (1960) commented on these values of loss tangent as being very good with the exception of the maximum value. He felt that on the basis of more recent studies the actual peak value may be about .08 to .09.

Experimental values of storage modulus and loss tangent of Plexiglas for several different frequencies were identical to published values within the limits of experimental error. This also served as an additional check on the theory used since the published values were found using a non-resonant technique.

In general, Young's modulus and the storage modulus were very similar in numerical value. The storage modulus was slightly larger, however, depending on the amount of damping present in the system. The storage modulus was more sensitive to changes in the frequency of the applied stress than other viscoelastic parameters measured for all materials tested. The storage modulus increased with increases in frequency. In addition, the storage modulus

increased much faster over a given frequency range for materials having higher loss tangents such as bark. For example, the storage modulus of bark having a loss tangent of about .15, increased from about 10,000 pounds per square inch at 10^{-3} cycles per second to over 40,000 pounds per square inch at about 30 cycles per second. The storage modulus for green wood with a loss tangent of about 0.04 only increased from about 500,000 pounds per square inch to 700,000 pounds per square inch over a slightly larger frequency range. The loss tangent is a ratio of the loss modulus to the storage modulus. Thus the loss tangent is directly proportional to the energy loss owing to heat and internal friction at a given frequency. This is a direct non-dimensional ratio of the amount of damping in the material. At medium frequencies, in the free vibration range, this ratio for the bark is about four times larger than that for the green wood. The amount of energy lost in a cycle may also be compared on the basis of the loss tangent δ by the relations

$$\text{Energy Loss Factor} = \frac{\Delta W}{W} = 2\pi \operatorname{Tan} \delta = 2\Delta = 4\pi\eta'$$

where W is the work done on the specimen. Therefore for bark the energy recovered and lost in a half cycle was about 55 and 45 per cent respectively and about 88 and 12 per cent respectively for green wood. Thus for a given stress level bark absorbs about four times as much energy as wood. However, in actual bending of a tree limb the

stress levels of the bark and wood are not the same, but are directly dependent on the respective moduli of elasticity and the distance from the neutral bending axis. At the outer fibers of the wood the elongations for the wood and bark would be about the same. In this case stresses produced in the bark and wood would be directly proportional to the vector sum of the loss and storage moduli.

In actual values the storage modulus of the bark is quite small being only 1/50 to 1/15 of that of wood. However, owing to the large difference in the loss tangents the loss modulus of bark is almost 1/3 that of wood depending on the frequency as shown in Table 7. The loss tangent and the storage modulus were also found to be somewhat sensitive to frequency. However, the direction of the change did not depend on the direction of change frequency, but was apparently dependent on the type of material being tested. For example, for an increase in frequency the storage modulus in green wood and white pine increased while in bark it remained constant and in Plexiglas it actually decreased. However, Koppelmann (1958) found that for frequencies below 45 cycles per second the storage modulus and the loss tangent increase with increases in frequency.

Therefore, it is apparent that changes in storage modulus in general depend on the direction of the frequency change, the material and the relative position in the frequency bandwidth.

TABLE 7.--Storage modulus, loss modulus, and loss tangent for bark and other materials tested at different frequencies of applied stress.

	Specimen	Moisture d.b.	Quasi-Static Rate = 0.05 ipm Frequency x10⁻³ cps.	Quasi-Static Rate = 0.05 ipm E'(ω=1/t) psi.	Free Vibration Frequency cps.	Free Vibration E'(ω) psi.	Free Vibration E"(ω) psi.	Free Vibration Loss Tangent	Forced Vibration Frequency cps.	Forced Vibration E'(ω) psi.	Forced Vibration E"(ω) psi.	Forced Vibration Loss Tangent
BARK TISSUE (Montmorency Cherry)	B1	146	1.26	12,010	7.4	30,100	4,780	.15	*	*	*	*
	B2	138	1.87	11,400	5.8	25,500	5,068	.17	*	*	*	*
	B3	132	2.12	12,210	7.5	37,980	4,513	.12	34	32,200	5,049	.13
	B4	127	1.20	9,[illegible]	[illegible].35	25,790	3,173	.12	29	32,200	7,716	.24
	B5	113	1.52	21,720	6.45	40,020	6,398	.16	*	*	*	*
GREEN WOOD (Montmorency Cherry)	G1	39	2.45	466,800	[illegible].4	493,900	14,800	.030	276	668,500	35,780	.054
	G2	38	2.0	525,800	[illegible].5	572,700	19,560	.034	290	741,000	35,700	.048
PLEXIGLAS	P1	n.a.	5.3	422,800	[illegible].6	579,000	44,300	.077	205	693,700	40,590	.060
	P2	n.a.	5.05	415,800	[illegible].3	595,100	49,000	.082	209	734,600	49,180	.067
WHITE PINE	W1		4.85	1,074,000	[illegible].5	1,162,000	20,550	.018	n.m.	n.m.	n.m.	n.m.
	W2		5.25	1,143,000	[illegible].3	1,186,000	29,160	.025	501	1,339,000	56,090	.042
	W3		4.84	1,164,000	n.m.	n.m.	n.m.	n.m.	n.m.	n.m.	n.m.	n.m.
ALUMINUM (alloy)	A1	n.a.	9.9	9,295,000	n.m.	n.m.	n.m.	n.m.	+	+	+	+
	A2	n.a.	14.0	9,[illegible]00,000	1[illegible].5	9,483,000	188,220	.019	+	+	+	+

n.a. - not applicable
n.m. - not measured
\+ - exceeded power limits of driver
* - fundamental resonance below frequency response of oscillator

In terms of models Plexiglas below 10 cycles per second behaves like a Kelvin material (spring and dashpot in parallel) where the loss tangent equals $\tau\omega$ and a Maxwell model above 10 cycles per second where the loss tangent equals $1/\tau\omega$. The response of these two models could be replaced by a Standard Solid model consisting of a spring and Maxwell element in parallel. By adjusting the constants of this model to have a peak value for loss tangent of about .10 at 45 cycles per second, a better approximation for this material may be made. The loss tangent could be even better by making $\tau = \tau(\omega)$ in the Standard Solid. In the data available for the green wood the loss modulus increases with frequency. This gives the impression that the viscous mechanism is forced to undergo displacement which produces a correspondingly large dissipation energy. This behavior is similar to that of the Kelvin model. Behavior of this type is also somewhat similar to that of cross linked polymers. In these cases the loss tangent reaches peak values at frequencies of about 10^5 cycles per second.

The behavior of the bark was in direct contrast to that of the green wood. The loss modulus of the bark was relatively flat over the frequency range and was relatively large compared to the storage modulus. The low elasticity and high loss modulus of bark is in keeping with one of its main functions which is acting as a shock absorbing protective

tissue for the tree. However, as shown in Figure 22 the storage modulus of bark increases spectacularly over the values at low frequencies. Therefore the bark becomes much stiffer and more subject to damage from forces applied at higher frequencies. This characteristic large increase in storage modulus with lesser increases in loss modulus, in bark tissue is similar to the behavior of polyvinyl acetate. Ferry (1961) describes this polymer as an amorphous polymer of high molecular weight. Over a similar frequency range the storage modulus for this material follows an "S" shaped curve such as suggested in this case for bark in Figure 22.

Surprisingly the storage modulus was most affected by changes in moisture content of the bark specimens. Ideally in a viscoelastic system represented by springs and dashpots one would expect little change in the storage modulus and an increase in the storage modulus for a decrease in moisture content. Actually the behavior is equivalent to the stiffening of the spring in the model with decreasing moisture content. In this respect the storage modulus appears to be a better indicator of moisture change than the loss tangent or the loss modulus. This points out the validity of studies which have been conducted in the past attempting to relate moisture content in biological materials such as wood and plant fibers to Young's modulus of elasticity.

Significance of Results

The results in this Thesis have defined some of the more important physical constants necessary to mathematically describe the behavior of bark and greed wood to applied stresses. To determine these constants, viscoelastic models were proposed to represent the material. The time dependent model constants were determined from experimental results. Variability in the constants between samples resulted from experimental error and variations between samples. Tests were conducted over a range of three fixed frequencies for each specimen tested.

As a next step in this investigation a complete constitutive equation which considers frequency (strain rate) and moisture content should be stated. Actually with the constants known for a particular frequency this equation has already been stated in this Thesis by the expressions for the complex modulus. It remains, however, to adjust this expression to fit a range of frequencies and moisture contents.

A further step in this investigation, of course, would be finally to apply these equations to a two dimensional study of a vibrating limb. This problem must be formulated to include the taper of the limb and satisfy the boundry conditions at the wood-bark interface. This would provide a direct experimental check on the original constants, the constitutive equations and the stress analysis solution for the limb.

SUMMARY

This study was initiated to study the mechanical behavior of fruit tree bark to applied stresses. Since the green wood is closely associated with the bark in the tree limb green wood was also included. Also since, during mechanical harvesting different frequencies of vibration are used, the frequency of the applied stress was also considered. Tests were limited to a single variety and species; Montmorency Cherry, Prunus Crasus.

All tests were conducted under controlled temperature and humidity conditions in a testing chamber. Maximum strength of bark specimens was determined from tensile loading in a pneumatic testing machine. Elastic and viscous properties of bark and green wood specimens were measured using elastic and viscoelastic flexure theory. Three loading techniques were used for the flexure tests. These tests were (1) loading at a slow, constant strain rate using a simple beam arrangement; (2) free vibration as a cantilever beam and (3) forced vibration as a simple beam. As a check on the theory and experimental technique several specimens of aluminum, Plexiglas, and white pine wood were included in these tests.

Approximate and exact equations for determining the viscoelastic modulus from dynamic flexure were derived. The accuracy of these equations was described graphically in terms of measured variables. From this it was possible to use the approximate equations with a negligible amount of error.

From a transverse microscopic section of bark the tissue appeared to be arranged in four major radial layers. These layers consisted of a functioning, and a spongy, non-functioning phloem, and two periderms which made up about 10, 65, 12, and 12 per cent of the total thickness respectively.

The strength of bark was very dependent on the direction of the applied force. Maximum longitudinal and tangential strengths for the three inner bark tissues were about 640 and 70 pounds per square inch respectively. The outer periderm strengths were about 980 and 3250 pounds per square inch in these respective directions. Longitudinal cambium shear strength was about 30 pounds per square inch.

The storage modulus of bark was very sensitive to frequency of the applied stress and varies from about 10,000 to 40,000 pounds per square inch over a frequency range of about 10^{-3} to 10^{-2} cycles per second. The storage modulus of green wood varied a lesser amount from about 500,000 to 700,000 pounds per square inch over a slightly larger frequency range. The loss tangents of bark and wood were about .15 and .04 respectively.

CONCLUSIONS

1. Both bark and green wood exhibit common viscoelastic effects such as non-linear loading curves, stress relaxation under load and high internal damping.
2. For the purpose of mechanical study bark may be divided into four major radial layers; a cambium, a nonfunctioning phloem and two periderms.
3. Strength properties of bark tissues are directional. Maximum strength for the inner bark tissues are about 640 and 70 pounds per second in the longitudinal and tangential directions respectively. The outer periderm strength is about 980 and 3250 pounds per square inch respectively, in the same direction.
4. Average longitudinal shear strength was about 30 pounds per square inch as measured on July 8, 1965. However, it is suspected that this property is subject to large changes owing to moisture content and seasonal activity of the tree.
5. Viscoelastic flexure theory and testing techniques can be successfully applied to measure the behavior of bark and green wood.
6. The storage modulus of bark was quite low compared to green wood and increased quite rapidly with increases

in frequency of the applied stress from about 10,000 to 40,000 pounds per square inch. Over a similar frequency range the storage modulus varied from about 500,000 to 700,000 pounds per square inch.

7. It is desirable to have controlled temperature conditions in a testing chamber. The most effective method of preventing moisture loss is rapid testing after collection.

REFERENCES

REFERENCES

Adrian, P. A. and R. B. Fridley.
1963 Shaker-Clamp Design as Related to Allowable Stresses of Tree Bark. American Society of Agricultural Engineers Paper Number 63-121. Saint Joseph, Michigan.

Alfrey, Turner Jr.
1948 Mechanical Behavior of High Polymers. Interscience Publishers, Inc., New York, N. Y.

Bair, G.
1964 Static and Dynamic Modulus of Elasticity of Hardboard. Unpublished M. S. Thesis (Forest Products). The Michigan State University, East Lansing, Michigan.

Baumeister, T. (editor)
1958 Mark's Mechanical Engineers' Handbook. Sixth Edition. McGraw-Hill Book Co. Inc., New York, N. Y.

Bland, D. R.
1960 Theory of Linear Viscoelasticity. Pergamon Press, New York, N. Y.

Bland, D. R. and E. H. Lee.
1955 Calculation of the Complex Modulus of Linear Viscoelastic Materials from Vibrating Reed Measurements. Journal of Applied Physics. 26(12): 1947.

Brown, G. C.
1965 Some Factors Affecting the Longitudinal Shear of Bark From Fruit Tree Limbs, Unpublished M. S. Thesis (Agricultural Engineering). The University of California, Davis, California.

Chaney, D. H.
1964 Canker Disease-Setback for Mechanical Harvesting. Western Fruit Grower. 8(6):23.

Chang, F. S. C.
1964 Stress Relaxation and Hysteresis at Various Strain Rates. Journal of Applied Polymer Science. 8:37.

Church, Austin H.
1964 Mechanical Vibrations. John Wiley and Sons, Inc., New York, N. Y.

Devay, J. E., Lukezic, F. L., English, H., Uriu K., and C. J. Hansen.
1962 Ceratocystis Canker. California Agriculture. 16:2.

Esau, Katherine.
1965 Plant Anatomy. John Wiley and Sons, Inc., New York, N. Y.

Ferry, John D.
1961 Viscoelastic Properties of Polymers. John Wiley and Sons Inc., New York, N. Y.

Finney, E. E.
1963 The Viscoelastic Behavior of the Potato, Solanum Tuberosum, under Quasi-Static Loading. Unpublished Ph. D. Thesis (Agricultural Engineering). The Michigan State University, East Lansing, Michigan.

Finney, E. E., Hall, C. W. and G. E. Mase.
1964 Theory of Linear Viscoelasticity Applied to the Potato. Journal of Agricultural Engineering Research. 9(4):307.

Frey-Wyssling, Albert.
1952 Deformation and Flow in Biological Systems. Interscience Publishers, Inc., New York, N. Y.

Goens, E.
1931 Uber die Bestimmung des Elastizitasmodulus von Staben mit Hilfe von Biegungsschwingungen. Annalen der Physik. 11(6):42.

Halderson, J. L.
1963 Fundamental Factors in Mechanical Cherry Harvesting. American Society of Agricultural Engineers Paper Number 63-120. Saint Joseph, Michigan.

Hearmon, R. F. S.
1958 The Influence of Shear and Rotary Inertia on the Free Flexural Vibration of Wooden Beams. British Journal of Applied Physics. 9(10):381.

Heil, H. G. and W. H. Bennett.
1939 Fundamental Principles of Physics. Prentice-Hall, Inc., New York, N. Y.

Heyn, A. N. J.
1940 The Physiology of Cell Elongation. Botany Review. 6:515.

Hodgman, C. D. (editor)
1952 Handbook of Chemistry and Physics. 34th Edition. Chemical Rubber Publishing Co., Cleveland, Ohio.

Horio, M. and S. Onogi.
1951 Forced Vibration of Reed as a Method of Determining Viscoelasticity. Journal of Applied Physics. 22(7):977.

Kollmann, F. and H. Krech.
1960 Dynamiche Messung der elastischen Holzeigenschaften und der Dampfung. Holz Als RoH-Und Werkstoff.

Koppelmann, J.
1958 Uber die Bestimmung des dynamischen Elastizitats-modulus und dynamischen Schubmodulus im Frequenzbereich von 10^{-5} bis 10^{-1} Hz. Rheology Acta. 1:20.

Meyer, B. S., Anderson, D. B. and R. H. Bohning.
1963 Introduction to Plant Physiology. D. Van Nostrand Co., Inc., New York, N. Y.

Meyer, K. H.
1950 Natural and Synthetic High Polymers. Interscience Publishers, Inc., New York, N. Y.

Mohsenin, N. N. and H. Gohlich.
1962 An Engineering Approach to Evaluation of Textural Factors in Fruits and Vegetables. American Society of Agricultural Engineers, Paper Number 62-321. Saint Joseph, Michigan.

Nolle, A. W.
1948 Methods for Measuring Dynamic Mechanical Properties of Rubber-Like Materials. Journal of Applied Physics. 19(8):753.

Picket, G.
1945 Equations for Computation of Elastic Constants from Flexural and Torsional Resonant Frequencies of Vibration of Prisms and Cylinders. Proceedings of the American Society for Testing Materials. 45:846.

Roelofsen, P.
1959 The Plant Cell Wall. Handbuch der Pflanzenatomie. 3(4):58.

Schneider, H.
1945 The Anatomy of Peach and Cherry Phloem. Bulletin of The Torrey Botanical Club. 72(2):137.

Sienko, M. J. and R. A. Plane
1961 Chemistry. McGraw-Hill Book Co., Inc., New York, N. Y.

Thompson, W. T.
1965 Vibration Theory and Applications. Prentice-Hall, Inc., Englewood Cliffs, New Jersey.

Timoshenko, S. P.
1921 On the Correction for Shear of the Differential Equation for Transverse Vibrations of Prismatic Bars. Philosophical Magazine. 41:744.

Timoshenko, S. K.
1922 On the Transverse Vibrations of Bars of Uniform Cross-Section. Philosophical Magazine. 43:125.

Timoshenko, S. K.
1955 Vibration Problems in Engineering. D. Van Nostrand Co., Inc., New York, N. Y.

Wood Handbook Number 72.
1955 Forest Products Laboratory, U. S. Department of Agriculture. Government Printing Office, Washington, D. C.

Zoerb, G. C. and C. W. Hall.
1960 Some Mechanical and Rheological Properties of Grains. Journal of Agricultural Engineering Research. 5(1):83.

APPENDIX

Equations for Error Using the Approximate Solutions

The per cent error for storage and loss moduli can be calculated by the equation

$$\text{per cent Error} = 100\ (1-E_A/E_E) \tag{46}$$

where E_A is the approximate value of the loss or storage modulus and E_E is the exact value. Since a loss and storage modulus may be calculated for both forced and free vibration, four error terms will be possible. These equations may be easily derived from equations 28, 31, 34, 35, 38, 39, 42, and 43. As a first step ω_n in the exact equations was replaced by ω_{nd} using equation 38. As a typical example of this equation 39 would become

$$E''(\omega) = H\omega_{nd}^2 \frac{(\sqrt{1-\lambda^2}-1)}{\sqrt{2-\sqrt{1-\lambda^2}}}$$

By using equation 46 the per cent error may be represented by: for forced vibration,

$$\text{Per Cent Error}\ [E'(\omega)] = 100\ [1-(1+\beta^2/2)(2-\sqrt{1-\lambda^2})] \tag{47}$$

$$\text{Per Cent Error}\ [E''(\omega)] = 100\ \left[1-\frac{\beta\sqrt{2-\sqrt{1-\lambda^2}}}{\sqrt{1-\lambda^2}-1}\right] \tag{48}$$

and for free vibration,

$$\text{Per Cent Error}\ [E'(\omega)] = 100\ \left[1-\frac{(1+\alpha^2/2)}{(1-2/(1+4/\alpha^2)}\right] \tag{49}$$

$$\underset{\text{Error}}{\overset{\text{Per Cent}}{}} [E''(\omega)] = 100\,[1-\alpha\cdot\sqrt{1-2/(1+4/\alpha^2)}\cdot\sqrt{4/\alpha^2+1}] \tag{50}$$

where $\beta = \omega/\omega_{nd}$, $\lambda = \omega/\omega_n$ and $\alpha = \Delta/\pi$.

However, these error terms are somewhat involved and the error must be recalculated each time when the value of β or α increases. In addition, equations 47 and 48 require values of ω_n which are unknown. Therefore it was decided that graphical presentation of error for a range of β and Δ would be more useful. In order to compare the accuracy of the approximate equations in forced and free vibrations values of β and Δ were generated using the same values of the damping ratio, η'. Values were generated for η' in increments of .01 as η' varied from zero to 0.700. The error equations for these calculations were: for forced vibrations,

$$\underset{\text{Error}}{\overset{\text{Per Cent}}{}} [E'(\omega)] = 100\,(1-\,(1 + R_2^2/2)\,B^2) \tag{51}$$

$$\underset{\text{Error}}{\overset{\text{Per Cent}}{}} [E''(\omega)] = 100\,(1 - A) \tag{52}$$

and for free vibrations,

$$\underset{\text{Error}}{\overset{\text{Per Cent}}{}} [E'(\omega)] = 100(1-\,(1 + D_3^2/2)B^2) \tag{53}$$

$$\underset{\text{Error}}{\overset{\text{Per Cent}}{}} [E''(\omega)] = 100(1-\,B/D) \tag{54}$$

where

$$B = \sqrt{1 - 2\eta'^2}$$

$$A = \sqrt{1 + \eta'^2}$$

$$D = \sqrt{1 - \eta'^2}$$

$$R_2 = 2\,\lambda'\,A/B = \Delta\omega/\omega_{nd}$$

$$D_3 = 2\,\eta'/D = \Delta$$

These error terms as well as the true and approximate values of the damping ratio, η', are presented in Table A1.

TABLE A1.--Values of the damping ratio, η', the frequency ratio, $\Delta\omega/\omega_{nd}$, the logarithmic decrement, Δ, and the per cent error in the loss and storage moduli resulting from using the approximate equations which assume small values of damping. (Negative error values indicate the approximate value is larger than the exact value.)

	Forced Vibration				Free Vibration			
True Damping Ratio	Damping Ratio (Calculated)	Frequency Ratio (Measured)	Per Cent Error for E'(ω)	Per Cent Error for E"(ω)	Damping Ratio (Calculated)	Logarithmic Decrement (measured)	Per Cent Error for E'(ω)	Per Cent Error for E"(ω)
0.0000	0.0000	0.0000	0.00	0.00	0.0000	0.0000	0.00	0.00
0.0100	0.0100	0.0200	-0.00	-0.00	0.0100	0.0200	0.00	0.00
0.0200	0.0200	0.0400	-0.00	-0.02	0.0200	0.0400	0.00	0.02
0.0300	0.0300	0.0600	-0.00	-0.04	0.0300	0.0600	0.00	0.04
0.0400	0.0401	0.0801	-0.00	-0.07	0.0400	0.0800	0.00	0.08
0.0500	0.0501	0.1003	-0.00	-0.12	0.0500	0.1001	0.00	0.12
0.0600	0.0603	0.1206	-0.00	-0.17	0.0601	0.1202	0.00	0.18
0.0700	0.0705	0.1410	-0.00	-0.24	0.0701	0.1403	0.00	0.24
0.0800	0.0807	0.1615	-0.00	-0.31	0.0802	0.1605	0.00	0.32
0.0900	0.0911	0.1822	-0.01	-0.40	0.0903	0.1807	0.01	0.40
0.1000	0.1015	0.2030	-0.02	-0.49	0.1005	0.2010	0.02	0.50
0.1100	0.1120	0.2240	-0.02	-0.60	0.1106	0.2213	0.02	0.61
0.1200	0.1226	0.2452	-0.04	-0.71	0.1208	0.2417	0.04	0.73
0.1300	0.1333	0.2667	-0.05	-0.84	0.1311	0.2622	0.05	0.86
0.1400	0.1442	0.2884	-0.07	-0.97	0.1413	0.2827	0.07	1.00
0.1500	0.1552	0.3104	-0.10	-1.11	0.1517	0.3034	0.10	1.15
0.1600	0.1663	0.3327	-0.13	-1.27	0.1620	0.3241	0.13	1.32
0.1700	0.1776	0.3553	-0.16	-1.43	0.1725	0.3450	0.17	1.49

True Damping Ratio	Forced Vibration: Damping Ratio (Calculated)	Forced Vibration: Frequency Ratio (measured)	Forced Vibration: Per Cent Error for E'(ω)	Forced Vibration: Per Cent Error for E"(ω)	Free Vibration: Damping Ratio (Calculated)	Free Vibration: Logarithmic Decrement (measured)	Free Vibration: Per Cent Error for E'(ω)	Free Vibration: Per Cent Error for E"(ω)
0.1800	0.1891	0.3782	-0.20	-1.60	0.1829	0.3659	0.21	1.68
0.1900	0.2007	0.4015	-0.26	-1.78	0.1935	0.3870	0.27	1.89
0.2000	0.2126	0.4252	-0.32	-1.98	0.2041	0.4082	0.33	2.10
0.2100	0.2247	0.4494	-0.38	-2.18	0.2147	0.4295	0.40	2.33
0.2200	0.2370	0.4740	-0.46	-2.39	0.2255	0.4510	0.49	2.57
0.2300	0.2495	0.4991	-0.55	-2.61	0.2363	0.4726	0.59	2.83
0.2400	0.2623	0.5247	-0.66	-2.83	0.2472	0.4944	0.70	3.10
0.2500	0.2754	0.5509	-0.78	-3.07	0.2582	0.5164	0.83	3.39
0.2600	0.2888	0.5777	-0.91	-3.32	0.2692	0.5385	0.98	3.69
0.2700	0.3026	0.6051	-1.06	-3.58	0.2804	0.5608	1.14	4.01
0.2800	0.3166	0.6333	-1.22	-3.84	0.2916	0.5833	1.33	4.34
0.2900	0.3310	0.6621	-1.41	-4.12	0.3030	0.6060	1.54	4.70
0.3000	0.3458	0.6917	-1.62	-4.40	0.3144	0.6289	1.78	5.07
0.3100	0.3611	0.7222	-1.84	-4.69	0.3260	0.6521	2.04	5.46
0.3200	0.3767	0.7535	-2.09	-4.99	0.3377	0.6755	2.33	5.87
0.3300	0.3929	0.7858	-2.37	-5.30	0.3495	0.6991	2.66	6.30
0.3400	0.4095	0.8191	-2.67	-5.62	0.3615	0.7230	3.02	6.76
0.3500	0.4267	0.8535	-3.00	-5.94	0.3736	0.7472	3.42	7.24
0.3600	0.4445	0.8890	-3.35	-6.28	0.3858	0.7717	3.85	7.74
0.3700	0.4629	0.9259	-3.74	-6.62	0.3982	0.7965	4.34	8.27
0.3800	0.4820	0.9640	-4.17	-6.97	0.4108	0.8216	4.87	8.82
0.3900	0.5018	0.0036	-4.62	-7.33	0.4235	0.8470	5.45	9.41
0.4000	0.5224	1.0448	-5.12	-7.70	0.4364	0.8728	6.09	10.02
0.4100	0.5438	1.0877	-5.65	-8.07	0.4495	0.8990	6.79	10.67
0.4200	0.5662	1.1325	-6.22	-8.46	0.4628	0.9256	7.55	11.35

True Damping Ratio	Forced Vibration: Damping Ratio (Calculated)	Forced Vibration: Frequency Ratio (measured)	Forced Vibration: Per Cent Error for E'(ω)	Forced Vibration: Per Cent Error for E"(ω)	Free Vibration: Damping Ratio (Calculated)	Free Vibration: Logarithmic Decrement (measured)	Free Vibration: Per Cent Error for E'(ω)	Free Vibration: Per Cent Error for E"(ω)
0.4300	0.5896	1.1792	-6.83	-8.85	0.4762	0.9525	8.38	12.07
0.4400	0.6140	1.2281	-7.49	-9.25	0.4899	0.9799	9.29	12.82
0.4500	0.6397	1.2794	-8.20	-9.65	0.5039	1.0078	10.28	13.62
0.4600	0.6666	1.3333	-8.95	-10.07	0.5180	1.0361	11.35	14.46
0.4700	0.6950	1.3901	-9.75	-10.49	0.5324	1.0649	12.52	15.35
0.4800	0.7250	1.4501	-10.61	-10.92	0.5471	1.0943	13.79	16.29
0.4900	0.7568	1.5136	-11.52	-11.35	0.5621	1.1242	15.17	17.29
0.5000	0.7905	1.5811	-12.50	-11.80	0.5773	1.1547	16.66	18.35
0.5100	0.8265	1.6530	-13.53	-12.25	0.5929	1.1858	18.28	19.47
0.5200	0.8649	1.7298	-14.62	-12.71	0.6087	1.2175	20.04	20.66
0.5300	0.9061	1.8122	-15.78	013.17	0.6250	1.2500	21.94	21.93
0.5400	0.9505	1.9011	-17.00	-13.64	0.6415	1.2831	24.00	23.29
0.5500	0.9987	1.9974	-18.30	-14.12	0.6585	1.3171	26.23	24.74
0.5600	1.0511	2.1023	-19.66	-14.61	0.6759	1.3518	28.65	26.30
0.5700	1.1086	2.2173	-21.11	-15.10	0.6937	1.3874	31.27	27.97
0.5800	1.1721	2.3443	-22.63	-15.60	0.7119	1.4239	34.10	29.78
0.5900	1.2428	2.4857	-24.23	-16.10	0.7307	1.4614	37.17	31.73
0.6000	1.3223	2.6446	-25.92	-16.61	0.7500	1.5000	40.50	33.85
0.6100	1.4127	2.8255	-27.69	-17.13	0.7698	1.5396	44.10	36.17
0.6200	1.5171	3.0343	-29.55	-17.66	0.7902	1.5804	48.00	38.71
0.6300	1.6397	3.2795	-31.50	-18.19	0.8112	1.6224	52.23	41.52

True Damping Ratio	Forced Vibration: Damping Ratio (Calculated)	Forced Vibration: Frequency Ratio (measured)	Forced Vibration: Per Cent Error for E'(ω)	Forced Vibration: Per Cent Error for E"(ω)	Free Vibration: Damping Ratio (Calculated)	Free Vibration: Logarithmic Decrement (measured)	Free Vibration: Per Cent Error for E'(ω)	Free Vibration: Per Cent Error for E"(ω)
0.6400	1.7870	3.5740	-33.55	-18.72	0.8329	1.6658	56.83	44.66
0.6500	1.9691	3.9382	-35.70	-19.26	0.8553	1.7106	61.82	48.19
0.6600	2.2034	4.4069	-37.94	-19.81	0.8785	1.7570	67.23	52.22
0.6700	2.5227	5.0454	-40.30	-20.37	0.9025	1.8050	73.13	56.93
0.6800	2.9987	5.9974	-42.76	-20.92	0.9274	1.8548	79.54	62.59
0.6900	3.8343	7,6687	-45.33	-21.48	0.9532	1.9065	86.53	69.79
0.7000	6.0419	12.0838	-48.02	-22.06	0.9802	1.9603	94.15	80.19

MICHIGAN STATE UNIVERSITY LIBRARIES
3 1293 03071 1349